# FEASIBILITY STUDY OF THE PULSED GAS ANALYZER FOR TOXIC VAPOR DETECTION IN THE MINUTEMAN III ENVIRONMENT

By
W. W. Bursack
R. P. Keller
Honeywell Inc.

Technical Report (Interim)

AFRPL-TR-72-33

March 1972

THIS DOCUMENT APPROVED
FOR
PUBLIC RELEASE
& UNLIMITED DISTRIBUTION

AIR FORCE ROCKET PROPULSION LABORATORY
DIRECTOR OF LABORATORIES
AIR FORCE SYSTEMS COMMAND
EDWARDS, CALIFORNIA

# FEASIBILITY STUDY OF THE PULSED GAS ANALYZER FOR TOXIC VAPOR DETECTION IN THE MINUTEMAN III ENVIRONMENT

W. W. Bursack
R. P. Keller

THIS DOCUMENT APPROVED
FOR
PUBLIC RELEASE
& UNLIMITED DISTRIBUTION

AIR FORCE ROCKET PROPULSION LABORATORY
DIRECTOR OF LABORATORIES
AIR FORCE SYSTEMS COMMAND
EDWARDS, CALIFORNIA

# FOREWORD

This technical report was prepared by the Systems and Research Center of Honeywell Inc. and is submitted to the Air Force Rocket Propulsion Laboratory, Director of Laboratories, Air Force Systems Command, as Data Item B005 and B010 of Contract F04611-71-C-0059. The report covers the Phase I portion of the work relating to concept evaluation and feasibility demonstration. The report covers work performed between June 1971 and February 1972. This project is under the direction of Hugh E. Malone/RTSE.

The manuscript was released by the authors in March 1972. The number assigned to this report by Honeywell System and Research Center is 12658-FR1.

This technical report has been reviewed and is approved.

H. E. Malone
Rocket Propulsion Laboratory
Air Force Systems Command
Edwards, California 92523

Security Classification

**DOCUMENT CONTROL DATA - R & D**

*(Security classification of title, body of abstract and indexing annotation must be entered when the overall report is classified)*

1\. ORIGINATING ACTIVITY *(Corporate author)*

Honeywell Inc.
Systems & Research Division
2700 Ridgway Parkway, Minneapolis, Minnesota

2a. REPORT SECURITY CLASSIFICATION

Unclassified

2b. GROUP

NA

3\. REPORT TITLE

FEASIBILITY STUDY OF THE PULSED GAS ANALYSER FOR TOXIC VAPOR DETECTION IN THE MINUTEMAN III ENVIRONMENT

4\. DESCRIPTIVE NOTES *(Type of report and inclusive dates)*

Final Report

5\. AUTHOR(S) *(First name, middle initial, last name)*

William W. Bursack
Roger P. Keller

6\. REPORT DATE

10 March 1972

7a. TOTAL NO. OF PAGES

68

7b. NO. OF REFS

11

8a. CONTRACT OR GRANT NO.

F04611-71-C-0059

b. PROJECT NO.

c.

d.

9a. ORIGINATOR'S REPORT NUMBER(S)

12658-FR1

9b. OTHER REPORT NO(S) *(Any other numbers that may be assigned this report)*

AFRPL TR-72-33

10\. DISTRIBUTION STATEMENT

This document approved for public release and unlimited distribution.

11\. SUPPLEMENTARY NOTES

12\. SPONSORING MILITARY ACTIVITY

Rocket Propulsion Laboratory
Air Force Systems Command
Edwards AFB, California 93523

13\. ABSTRACT

A program was carried out for demonstrating the feasibility of a new concept for detecting and measuring monomethyl hydrazine (MMH) and nitrogen dioxide ($NO_2$) in the Minuteman III environment. A review of candidate methods for detection and measurement of MMH and $NO_2$ leakage vapors was made. The Pulsed Gas Analyzer (PGA) concept was selected and a feasibility demonstration was made using a laboratory model. This method was shown to have the required detectivity and measurement response for these materials. The sensitivity requirements of 0.2 ppm MMH and 5.0 ppm $NO_2$ were met. During the program, tests were run to evaluate performance of the laboratory model under extremes of humidity and temperature as well as in the presence of contaminate materials at relatively high concentrations. The effect of vehicle exhaust gas on the measurement of MMH and $NO_2$ was also noted. Measurement performance was not affected at temperatures up to 125°F. It was degraded at 0°F apparently because MMH and $NO_2$ partially condensed before entry into the measuring volume of the instrument. Application of heat to the sample line has not yet been tried. Measurement performance was not affected by the presence of several of the contaminates, but it was degraded when MMH and $NO_2$ were present simultaneously in the atmosphere (apparently because of the mutual reactivity of these materials). In some cases, performance was degraded by certain amines, acetaldehyde, and water vapor. Some of the interferences were suspected of being reactions between the chemicals present (e.g., MMH oxidizes in humid air). The logic scheme used for MMH and $NO_2$ detection was based on the use of only two mass numbers in the mass spectra of these materials. Additional logic may be added to denote measurement conditions compromised by the presence of contaminates. A proposed PGA breadboard configuration has been described.

**DD** FORM 1 NOV 65 **1473** REPLACES DD FORM 1473, 1 JAN 64, WHICH IS OBSOLETE FOR ARMY USE.

Security Classification

Security Classification

| 14. KEY WORDS | LINK A | | LINK B | | LINK C | |
|---|---|---|---|---|---|---|
| | ROLE | WT | ROLE | WT | ROLE | WT |
| Minuteman III | | | | | | |
| Toxic vapor | | | | | | |
| Pulsed gas analyzer | | | | | | |
| Monomethyl hydrazine | | | | | | |
| Nitrogen dioxide | | | | | | |

# ABSTRACT

A program was carried out for demonstrating the feasibility of a new concept for detecting and measuring monomethyl hydrazine (MMH) and nitrogen dioxide ($NO_2$) in the Minuteman III environment. A review of candidate methods for detection and measurement of MMH and $NO_2$ leakage vapors was made. The Pulsed Gas Analyzer (PGA) concept was selected and a feasibility demonstration was made using a laboratory model. This method was shown to have the required detectivity and measurement response for these materials. The sensitivity requirements of 0.2 ppm MMH and 5.0 ppm $NO_2$ were met. During the program, tests were run to evaluate performance of the laboratory model under extremes of humidity and temperature as well as in the presence of contaminate materials at relatively high concentrations. The effect of vehicle exhaust gas on the measurement of MMH and $NO_2$ was also noted. Measurement performance was not affected at temperatures up to 125°F. It was degraded at 0°F apparently because MMH and $NO_2$ partially condensed before entry into the measuring volume of the instrument. Application of heat to the sample line has not yet been tried. Measurement performance was not affected by the presence of several of the contaminates, but it was degraded when MMH and $NO_2$ were present simultaneously in the atmosphere (apparently because of the mutual reactivity of these materials). In some cases, performance was degraded by certain amines, acetaldehyde, and water vapor. Some of the interferences were suspected of being reactions between the chemicals present (e.g., MMH oxidizes in humid air). The logic scheme used for MMH and $NO_2$ detection was based on the use of only two mass numbers in the mass spectra of these materials. Additional logic may be added to denote measurement conditions compromised by the presence of contaminates. A proposed PGA breadboard configuration has been described.

# TABLE OF CONTENTS

# LIST OF ILLUSTRATIONS

## LIST OF ILLUSTRATIONS -- CONCLUDED

# SECTION I

# INTRODUCTION

The Minuteman III, fourth-stage, Post Boost Propulsion System contains monomethyl hydrazine (MMH) and nitrogen tetroxide (NTO), leakage of which constitutes an operational and physiological hazard. A concept for detection and measurement of these vapors in the Minuteman III environment has been proposed and feasibility has been demonstrated. The concept makes use of a pulsed-mode mass spectrometer which is tuned to specific mass numbers indicating the presence of MMH and the monomer form of nitrogen tetroxide - nitrogen dioxide ($NO_2$). Pulsed-mode sample introduction does away with the cumbersome pumping requirements of mass spectrometry while retaining its excellent analytical capabilities and the feature of direct conversion of molecular population to electric current. These qualities have now been demonstrated along with the capability for detecting the desired MMH and $NO_2$ threshold concentrations.

This document reports the results of a test program using a laboratory version of the Pulsed Gas Analyzer (PGA) and also notes a number of detection methods which were considered. (These have been discussed more fully in an interim project report.) The PGA laboratory model was designed to demonstrate function rather than geometric configuration. It now appears reasonable to project a subsequent PGA breadboard model configuration. This has been done in the last section of this document.

During the program consideration was given to the effects of humidity extremes, temperature extremes, and the presence of contaminate gases (including internal combustion engine exhaust) on MMH and $NO_2$ detection and measurement. A summary of the test findings is given in Sections VII and VIII, with recommendations for further testing in Section IX. Issues requiring further resolution in light of Minuteman III operations and atmospheric environment relate to possible contaminate concentrations, sampling of small concentrations of leakage vapors at low temperatures, the oxidation of MMH in humid atmospheres, and the concern for detecting simultaneous MMH and $NO_2$ leaks.

## SECTION II

## REQUIREMENTS FOR TOXIC VAPOR DETECTION IN THE MINUTEMAN III ENVIRONMENT

The Minuteman III, fourth-stage, Post Boost Propulsion System (PBPS) contains the stored, liquid bipropellant combination of nitrogen tetroxide (NTO) and monomethyl hydrazine (MMH). Leakage of either of these toxic propellants constitutes an operational and personnel hazard. There is a requirement to monitor the surrounding environment for the vapors of these toxic propellants, as a warning of propellant leaks when operations are being performed on or around the PBPS. Detection of toxic vapors at concentrations below the level of olfactory recognition, with a suitable warning system permits prompt implementation of emergency procedures. This minimizes both hazards.

Vapor detection monitoring is required during PBPS transport, storage, and installation, and during silo operations, such as maintenance and repairs. The requirements for silo operations are probably most demanding, and a vapor detection system which meets the demands for silo operations, without interfering with operational functions, would probably be suitable to the other operations. To function effectively the toxic vapor detector should have a capability for continuous monitoring and scale readout, and provisions for the attachment of a recorder.

Because trace gases other than NTO and MMH may be present in the atmosphere, leakage vapor detection should not be compromised by their presence. Carbon monoxide, nitrogen oxides, and hydrocarbons are emissions produced by spark and compression ignition engines. These in turn can be converted to other compounds in atmospheric reactions. Still other trace gases may be produced by off-gassing of materials in the silo. The following atmospheric contaminants should not interfere with the detection of MMH and nitrogen dioxide ($NO_2$):

- Methane
- Carbon monoxide
- Hydrogen
- Freon 114 B-2
- Ammonia

In addition, representative aldehydes, ketones, and amines should not interfere. The possibility of simultaneous leaks of fuel and oxidizer should also be recognized.

The requirements for the toxic vapor detector's design and function are summarized in Table I. It is noted that high and low scale ranges are required for readouts of MMH and $NO_2$. The total readout range is from 0 to 100 ppm for MMH, and 0 to 500 ppm for $NO_2$. The minimum detection capability corresponds to the threshold limit values of 0.2 ppm for MMH and 5.0 ppm for $NO_2$. Readout response time (90 percent) is 1 minute, with initial response observable in 10 seconds.

The temperature and humidity requirements reflect climatic conditions of Minuteman III operation in which the toxic vapor detector could be exposed to temperatures from -40°F to +150°F and to relative humidities from 5% to 95%

The toxic vapor detector is to be portable, having a weight less than 30 pounds for transport by one man. The detector is to have provision for operator verification of operability and a minimum of 500 hours mean time between failure (MTBF) operating life. In addition to visual readouts of MMH and $NO_2$ concentrations, the toxic vapor detector is to have visual and audio alarms whose set points can be adjusted, and which may be overridden and reset (Table I).

Feasibility demonstration of the Pulsed Gas Analyzer as an MMH/$NO_2$ vapor detector involves compliance to the requirements for:

- Visual readouts of concentrations using high and low scale ranges
- Minimum concentrations detection
- Temperature and humidity extremes
- Noninterference by contaminates
- Measurement response time

Such requirements as size and weight, incorporation of alarms and self-contained power supply, and operability verification are to be met in subsequent breadboard and prototype configurations of the toxic vapor detector.

## Table I. Instrumentation Requirements for Minuteman III Toxic Vapor Detection

| Feature or Function | Value or Design/Performance Citation |
|---|---|
| 1.0 Measurement Function | |
| 1.1 Range | MMH 0 - 2 ppm and 0 - 100 ppm<br>$NO_2$ 0 - 10 ppm and 0 - 500 ppm |
| 1.2 Accuracy | MMH 0, +0.2 ppm and ± 10%<br>$NO_2$ -1, +2 ppm and ±10% |
| 1.3 Detectivity | MMH 0.2 ppm<br>$NO_2$ 5.0 ppm |
| 1.4 Response | 10 seconds (show)<br>60 seconds (90%) |
| 1.5 Specificity | Meet requirements in presence of normal air and background contaminates |
| 1.6 Selectivity | MMH, $NO_2$ |
| 1.7 Environmental Stability: | |
| +40° to +90°F | Meet requirements |
| 0° to +125°F | ±20% accuracy |
| -40° to +150°F | Meet requirements after exposure |
| 0 to 95% R.H. | Meet requirements |
| 2.0 Fieldworthy Design | |
| 2.1 Size | |
| 2.2 Weight | < 30 lb |
| 2.3 Portability | 1-man carry; silo hoist |
| 2.4 Ruggedness | |
| 2.5 Environment dependent | |
| 2.6 Hazard generation | |
| 3.0 Operability | |
| 3.1 Procedural simplicity | |
| 3.2 Self-check | Verification of operability |
| 3.3 Readout/control features | Flashing light; audio alarm<br>Variable, manually-set alarm<br>Manual override; audio alarm<br>Automatic reset; audio alarm<br>Manual reset; visual alarm<br>Scale readability<br>Recorder output<br>6-hour recording capability |
| 3.4 Operable during portage | Required |
| 3.5 False alarm rate | Negligible |
| 4.0 Maintenance | |
| 4.1 Overhaul frequency | |
| 4.2 Overhaul simplicity | |
| 4.3 Calibration certification | Periodically |
| 4.4 Expendables use | |
| 4.5 Parts replacement frequency | |
| 4.6 System life | 3-year (minimum); 10 year (desired)<br>500-hour MTBF |
| 5.0 Power Requirements | 115 vac ± 10%; 60 ± 3 Hz; single-phase<br>8-hour operation without external power<br>Simultaneous operation and recharge<br>Recharge power: 115 vac ± 10%, 60 ± 3; Single-phase<br>Recharge time (non-operating): 16 hours<br>Battery charge indicator |

# SECTION III

# POSSIBLE DETECTION METHODS AND SELECTION OF THE PULSED GAS ANALYZER CONCEPT

A study of trace gas detection methods was made in light of the Minuteman III toxic vapor detection requirements. This study, Interim Project Report No. 12658-IR1, has substantiated the choice of the Pulsed Gas Analyzer (PGA) as the toxic vapor detection method.

The requirements for vapor detection in the Minuteman III environment have been listed in Table I. Detection methods evaluated against these requirements include:

- Condensation nuclei
- Electrochemical and wet chemical
- Electron impact spectrometer
- Gas chromatography
- Ionization techniques
- Liquid crystals
- Mass spectroscopy (PGA)
- Microwave spectroscopy
- Optical: Chemiluminescence
- Optical: Derivative spectrometer
- Optical: IR (closed cell)
- Optical: IR (long path)
- Optical: Raman
- Optical: Molecular correlation
- Optical: Ultraviolet
- Surface effect

The several detection methods are evaluated in Table II against the application requirements. Biological, liquid crystal, and surface-effect methods are shown to be insufficiently reduced to practice for consideration. The condensation nuclei, electrochemical and wet chemical, and chemiluminescent methods have been applied to $NO_2$, but presumably other methods would be required for MMH. For several methods requiring unique spectral signatures in detection (electron impact, microwave, derivative, Raman, molecular correlation), it is perhaps reasonable to assume that such uniqueness

# TABLE II. - LIMITATIONS OF DETECTION METHODS: MINUTEMAN III PVD APPLICATION

| Criteria / Methods | Measurement Function | | | | | | | | Fieldworthy Design | | | | | | Operability | | | | | Maintenance | | | | | | | | | |
|---|---|---|---|---|---|---|---|---|---|---|---|---|---|---|---|---|---|---|---|---|---|---|---|---|---|---|---|---|---|
| | Range | Accuracy | Detectivity | Response | Specificity | Selectivity | Stability | Environmental Stability(1) | Size | Weight | Portability | Ruggedness | Environment Dependent | Hazard Generation | Procedural Simplicity | Self-Check | Readout/Control Features | Operable at Portage | False Alarm Rate | Overhaul Frequency | Calibration Certification | Expendables Use | Parts Replacement Frequency | System Life | Power Requirements | Reduction to Practice | Cost | Producibility | |
| Biological Systems | | | | X | | | | X | | | | | | | | | | | | | | | | | | X | | | |
| Condensation Nuclei Detector | | | | X | X | | X | X | | | X | | | | | | | | | | | X | | | | (3) | | | |
| Electrochemical/Wet Chemical | | | | X | X | | X | X | X | X | X | | | | X | | | X | | X | | X | | | | (3) | | | |
| Electron Impact Spectrometer | | | X | | | | | | X | X | X | | | | X | | | | | | | | | | | (4) | | | |
| Gas Chromatography | | | X | X | | | | X | | X | X | | | | | | | | | | | X | | | | | | | |
| Ionization | | | | | X | | | | | | | | | X(2) | | | | | | | | X | | | | | | | |
| Liquid Crystals | | | | | | | | X | | | | | | | | | | | | | | | | | | X | | | |
| Mass Spectrometer/PGA | | | | | | | | | | | | | | | | | | | | | | | | | | | | | |
| Microwave Spectroscopy | | | X | | | | | | X | X | X | | | | | | | | | | | | | | X | (4) | | | |
| Optical: Chemiluminescence | | | | | | | | | X | X | X | | | | | | | | | | | | | | | (3) | | | |
| Optical: Derivative Spectrometer | | | X | | | | | | X | X | X | | X | | | | | | | | | | | | | (4) | | | |
| Optical: IR/Closed Cell | | | X | | X | | | | | | | | | | | | | | | | | | | | | | | | |
| Optical: IR/Long Path | | | X | | X | | | | | | X | | | | | | | | | | | | | | | | | | |
| Optical: Raman | | | X | | X | | | | | | X | | X | | | | | | | | | | | | | (4) | | | |
| Optical: Molecular Correlation | | | X | | | | | | | | | | X | | | | | | | | | | | | | (4) | | | |
| Optical: Ultraviolet | | | X | | X | | X | X | | | | | X | X(2) | | | | | | | | | | | | | | | |
| Surface Effect | | | | | | | | | | | | | | | | | | | | | | | | | | X | | | |

(1) Requires at least temperature regulation
(2) When flame is used
(3) Questionable for both $NO_2$ and MMH
(4) Spectral signature not established

could be arrived at, but these methods lack the required detectivity and have other shortcomings. In general, the optical methods lack detectivity and specificity. Those operating in the ultraviolet and visible ranges, or with weak phenomena (Raman), are also subject to interference from ambient radiance.

Ionization methods work well as detectors in gas chromatography where their lack of specificity is not a consideration. They require the use of expendables (carrier gas), and in one case there may be a potential fire/explosion hazard (flame ionization method). For these reasons ionization methods are not considered for Minuteman III. The lack of specificity also rules out the multi-agent detector - an ionization method not requiring a carrier gas.

Gas chromatography has excellent sensitivity and resolution using long separation columns, but these performance factors are degraded when the short columns of faster response, smaller instruments are used. In addition, the method is not considered because of its relatively long response time, lack of portability, and the need for expendables (carrier gas).

The size and weight limitations of mass spectrometry are overcome by using pulsed-mode operation. This mode of operation is expected to enhance the detectivity of this method, as well, by making available a dense gas sample for mass analysis.

Pulsed-mode operation of a quadrupole mass spectrometer (PGA) has been selected for the Minuteman III PVD application for the following reasons:

- Specificity - Both $NO_2$ and MMH can be detected and measured with the single instrument. In addition, the presence of contaminate or background gases can be ignored by selecting noninterfering mass numbers in detecting and measuring.

- Detectivity - The 1 to 10 ppm analytical capability of conventional quadrupole mass spectrometers is enhanced by pulsed-mode operation in expectation of the requirement for 0.2 and 5.0 ppm detectivity (MMH and $NO_2$, respectively). This will come about by using the momentarily high sample density in the ion source during sample pulsing.

- Accuracy - Ion currents associated with pulsed sample admission to an ion source are uniform and reproducible. The manipulation of ions in the mass analysis is controlled by electric fields whose frequencies and amplitudes are accurately controlled. Isotopic argon peaks are available for automatic calibration of the instrument using the argon level in the atmosphere as a reference.

- Response - The PGA provides real-time readout in the sense that mass analysis can be accomplished during the sampling interval (about 2 milliseconds). Sampling frequency can be as often as once per second.

- Stability - Good stability (long-term accuracy) in any trace gas detecting instrument requires consistent sample introduction and control of the measurement process. With the PGA, pulsed leak performance must provide the former and the constancy of electric circuit components the latter. Virtually no moving parts are used. The detection process involves well-controlled circuit performance rather than chemical reaction, flow control, radiation modulation, etc.

- Size, Weight, Portability - Size/weight projections for the PGA indicate a 0.1-cubic-foot volume and about 10 pounds weight (without battery). A nickel-cadmium battery would weigh from 10 to 15 pounds depending on the eventual power needs of the PVD. It is expected that the 30-pound goal for the final PVD configuration can be met. Since the unit would be entirely self-contained as well, it could be hand-carried in various locations throughout the Minuteman III complex.

- Amenability to Read-Out Requirements - Table II showed that no detection method has a limitation as regards provision for the required read-out functions (visual-audible alarms, overrides, resets, etc.). However, the PGA concept directly converts MMH and $NO_2$ molecule populations to electrical currents which can be readily manipulated. When outputs are indicated for these materials, sample and hold circuits are enabled. Analog outputs from these circuits are routed to the display circuits (metered indication of concentration, flashing alarm, audio alarm).

- State-of-Art - No breakthroughs in state of art are required to develop the PVD using the PGA concept. Quadrupole mass spectrometers have been in use for many years and are commercially available. The pulsed leak has been in use at Honeywell for several years as a metering device and vacuum laboratory tool. The electric-field ion pump has been used for several years at Honeywell for pumping electrically-suspended gyroscopes. Both electric-field and magnetic ion pumps are commercially available.

- Minimum Expendables Use - The PGA requires no carrier gas or chemical reagents. If sample line filtering is used for particulate or gas species (such as carbon dioxide), it is expected that material use would be of the order of a gram or so a day in continuous sampling - a quantity so small as to make only periodic filter replacement necessary.

- Life - Since the PGA is essentially free of moving parts, the wear-out problem is greatly minimized. The pulsed leak is the only component having a moving part, and pulsed leaks have been tested without failure over 10 million cycles when the test was arbitrarily terminated. Periodic overhaul every 6 or 12 months (depending on use) is expected to recondition or replace such parts as the filament, ion source electrodes and quadrupole rods, detector, and ion pump parts. Between overhaul periods, instrument calibration can be effected by monitoring isotope peaks of atmospheric components (such as argon 36 and 38) or by sampling assayed atmospheric mixtures.

- Versatility - The PGA concept is inherently versatile since it provides an ion current at each mass number in its operating range which can be inserted into electrical circuits for execution of logic and detection functions. Such functions can be carried out electrically with far greater facility than by altering or adding a basic sensing process (such as those using chemical reactions). One example of the usefulness of this attribute of the PGA is that of providing an automatic calibration feature using the argon 38 isotope peak.

## SECTION IV

## DETECTION RATIONALE FOR MMH/$NO_2$

An ideal situation for the detection of two different compounds by the PGA would be for them to have different molecular weights and for each molecular weight to have a value not shared by any other compound likely to be found under the conditions of operation and whose concentration in the atmosphere is subject to change. It would also be desirable for no ion fragments formed during ionization to have corresponding mass numbers.

MMH and $NO_2$ both have the same molecular weight (46). Therefore, monitoring only mass 46 would not provide information as to which compound was being sensed. However, the mass spectra of MMH shows that together with the parent ion peak at atomic mass unit (amu) 46, an abundant fragment ion appears at amu 45. The ratio of 46 peak height to 45 peak height is close to 2:1, and remains at this value over the ionization energy range 8.63 ev to 70 ev and over the concentration range 0.2 ppm to 100 ppm. Spectra showing MMH and $NO_2$ in air may be seen in Figures 1 and 2, respectively. Utilizing these facts, the system logic was designed to alternately monitor mass numbers 45 and 46. The $NO_2$ and MMH readouts are expressed as follows:

MMH = 2 x 45 peak

$NO_2$ = 46 peak - (2 x 45 peak)

$NO_2$ in the presence of MMH increases the 46/45 ratio to a value greater than 2. This excess is taken to be $NO_2$. Any signal at mass number 45 is attributed to MMH.

The fact that MMH and $NO_2$ have lower ionization potentials than the atmospheric gases and specified contaminates is fortunate. This permits both the use of selective ionization and mass filtering as techniques by which the PGA can detect these two materials in the presence of atmospheric gases and contaminates.

Ionization potential values of interest are given in Table III. This table shows that $NO_2$ and MMH have the lowest ionization potentials. The practical significance of this has been demonstrated by operating the ion source of the PGA laboratory model at low electron energies and noting the diminishment of the $CO_2$ peak at mass 44, elimination of the $CO_2$ isotopic 45 peak, and sufficient retention of the 45 and 46 peaks of MMH and the 46 peak of $NO_2$ to provide useful signals for their detection. At low levels of ionizing energy (14 ev) the atmospheric gases are not greatly ionized, but MMH and $NO_2$ are sufficiently ionized to obtain the required detection sensitivity. The pulsed mode of operation provides a momentarily high concentration of ions which offsets the effect of lowered ionization energy. The effects of lowering the

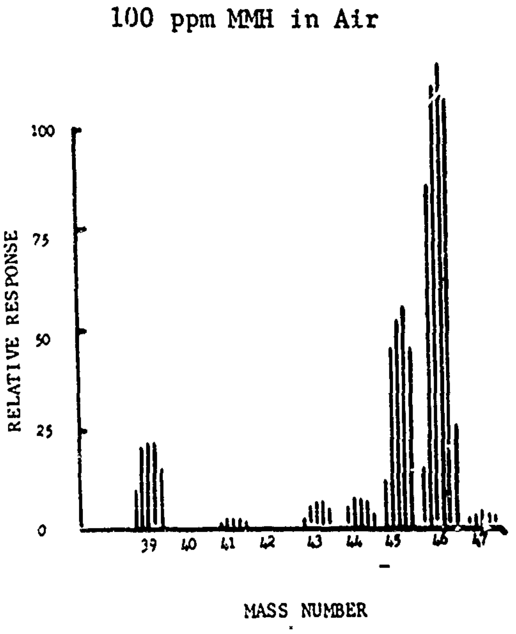

Figure 1. Replica of Pulsed Mode Spectra of MMH

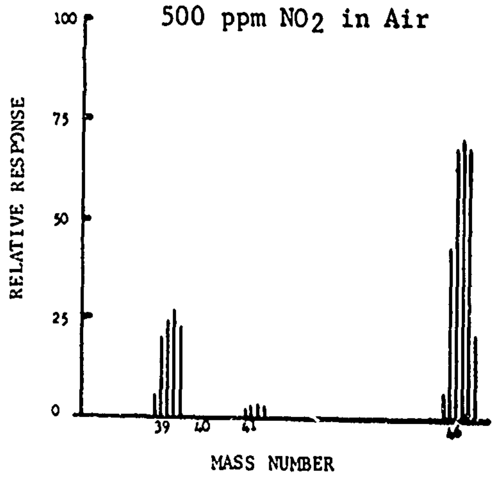

Figure 2. Replica of Pulsed Mode Spectra of $NO_2$

Table III. Ionization Potentials for Gases in the Minuteman Environment[1]

| Species | Ionization Potential (electron volts) | | |
|---|---|---|---|
| | Standard Atmosphere Species | Contaminates | PBPS Leakage |
| He | 24.48 | | |
| Ne | 21.56 | | |
| Ar | 15.75 | | |
| $N_2$ | 15.58 | | |
| CO | 14.01 | 14.01 | |
| Kr | 14.00 | | |
| $CO_2$ | 13.79 | | |
| $H_2$ | 13.59 | 13.59 | |
| $CH_4$ | 12.98 | 12.98 | |
| $N_2O$ | 12.89 | | |
| $O_3$ | 12.80 | | |
| $H_2O$ | 12.59 | | |
| $SO_2$ | 12.34 | | |
| Xe | 12.13 | | |
| $O_2$ | 12.07 | | |
| Formaldehyde | | 10.87 | |
| $I_2$ | 10.45 | | |
| Acetaldehyde | | 10.21 | |
| $NH_3$ | 10.15 | 10.15 | |
| Acetone | | 9.69 | |
| $NO_2$ | 9.78 | | 9.78 |
| MMH | | | 8.63 |

---

[1] Source: Kiser, R. W.: Introduction to Mass Spectrometry and Its Applications; Prentice-Hall (1965) [Freon 114 B-2, a contaminate, is not listed. Freons generally have high ionization potentials.]

electron energy are seen in Figure 3. This figure presents air spectra taken in the pulsed mode at electron energies of 12, 14, 16, and 18 ev. Note the absence of the water peak (18) and the presence of oxygen (32) on the 12 ev scan. On the 14-ev scan water (18) is higher than nitrogen (28), while on the 16-ev scan nitrogen is higher. Other examples may also be noted. Figure 4 shows air spectra with and without MMH at an electron energy of 15 ev Note the absence of amu peaks at 44 and 45 due to carbon dioxide - a potential interferant with MMH at amu 45.

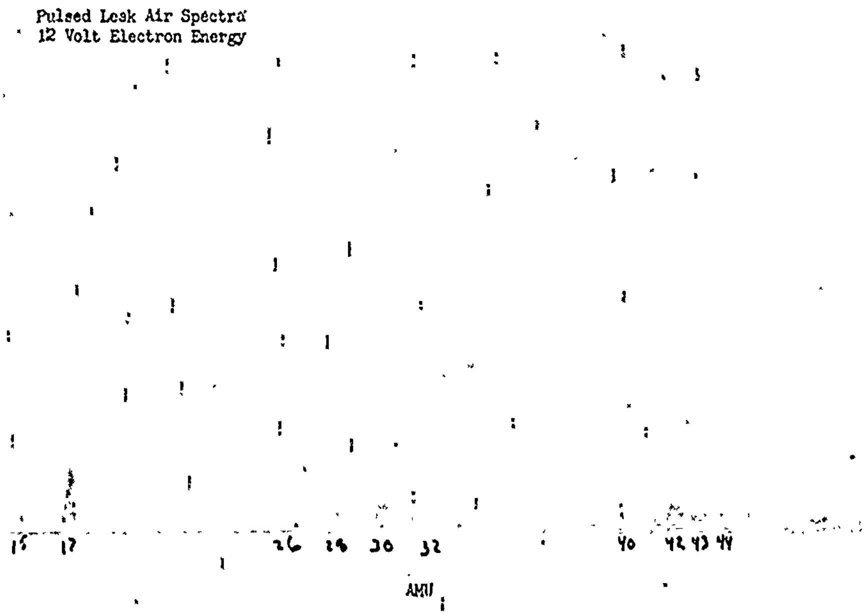

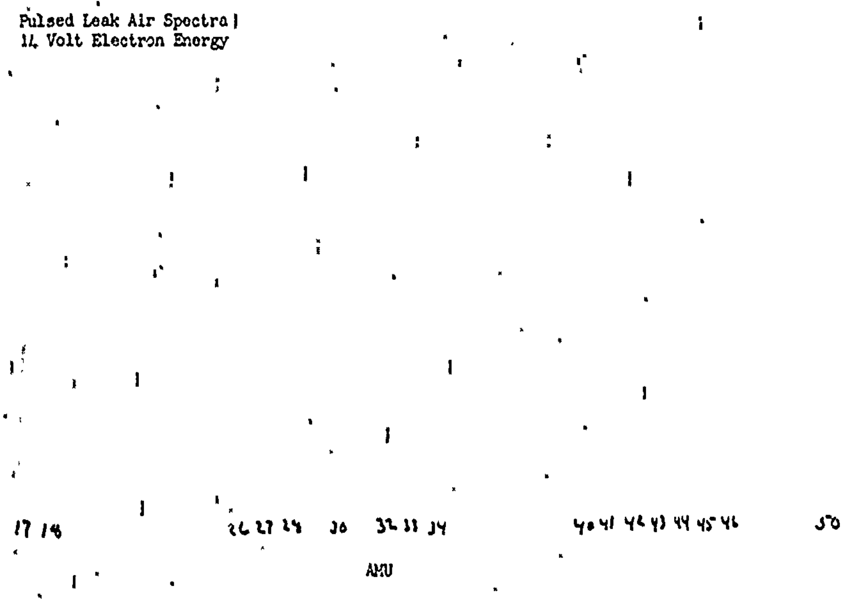

Figure 3. Pulsed Mode Spectra of Air at Different Electron Energies

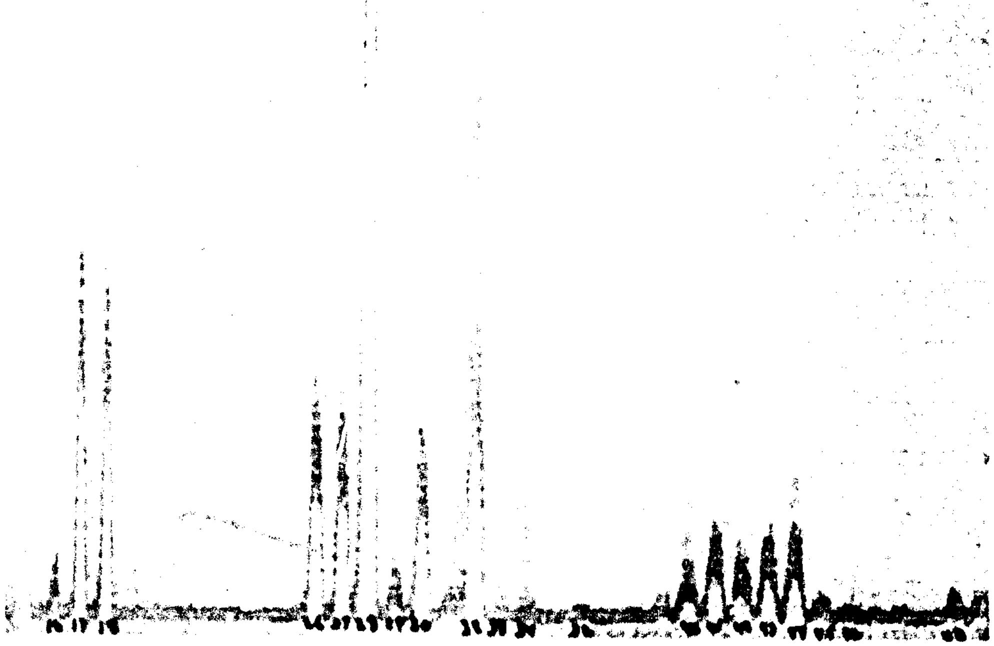

Pulsed Leak Air Spectra
16 Volt Electron Energy

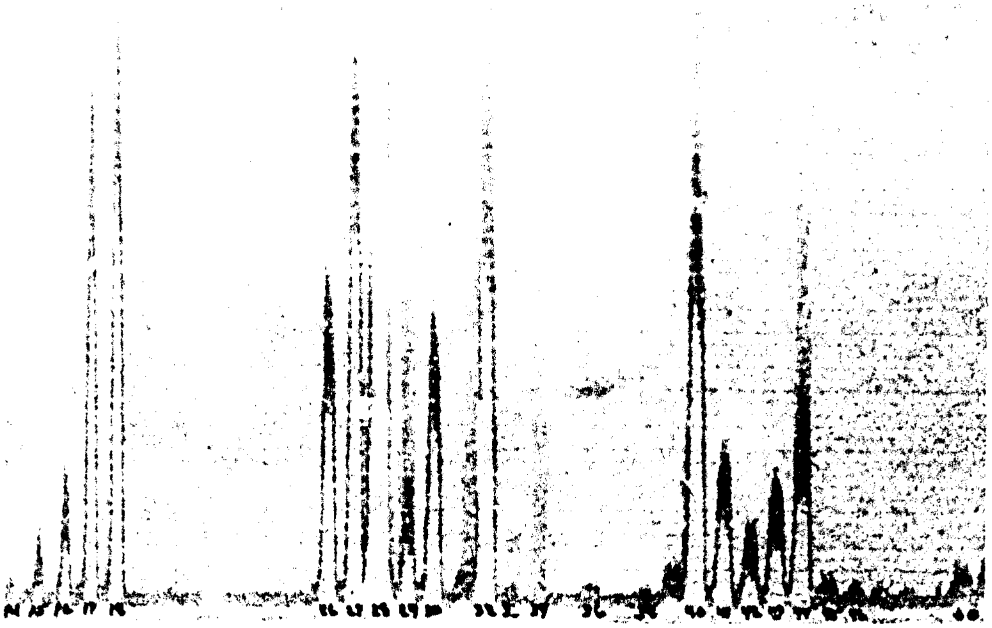

Pulsed Leak Air Spectra
18 Volt Electron Energy

Figure 3. Pulsed Mode Spectra of Air at Different Electron Energies (Concluded)

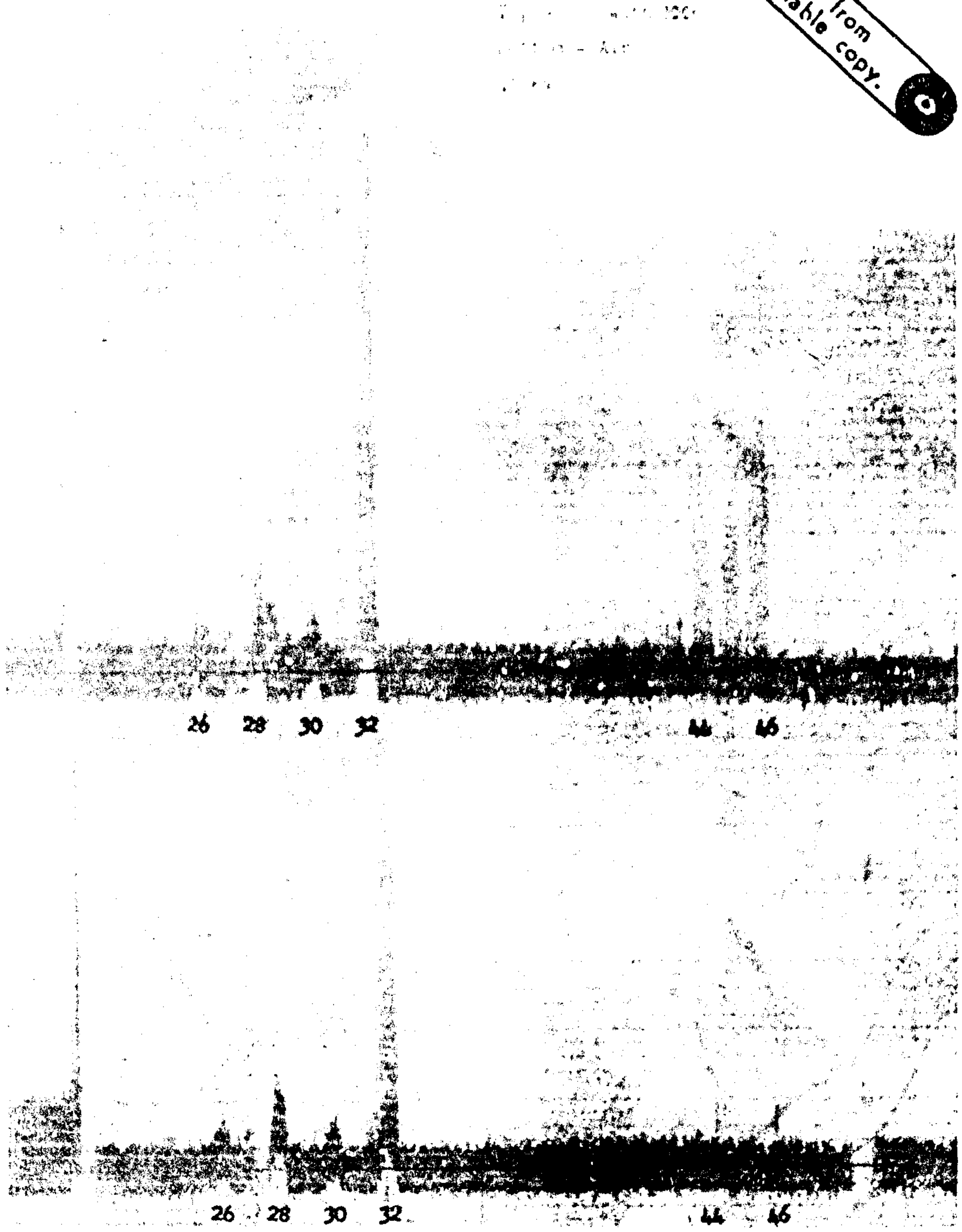

Figure 4. Air Spectra with and without MMH at 15V Electron Energy

# SECTION V

# DESCRIPTION OF THE PGA LABORATORY MODEL

The laboratory model, consisting essentially of laboratory-type equipment, has been used in demonstrating the feasibility of the PGA for detecting toxic vapors in the Minuteman III environment. Though designed to demonstrate function rather than geometric configuration, it appears reasonable now to project a subsequent breadboard model suitable for testing at AFRPL. The vacuum system and electronics of the laboratory and breadboard models would be sufficiently alike to expect similar measurement performance, at the same time anticipating the required degree of portability in the breadboard model through package design.

The PGA laboratory model consists of two functional parts; (1) the vacuum system and (2) the electronics system. These in turn may be subdivided as follows in further describing the Laboratory Model.

- Vacuum System
    - Quadrupole mass spectrometer
    - Ion pump
    - Pulsed leak
    - Roughing pump system
    - Ion gauge
- Electronics System
    - Quadrupole control
    - $MMH/NO_2$ control/display unit
    - Ion pump control
    - Ion gauge control

The laboratory model is shown in Figure 5. The vacuum system of the laboratory model is shown in Figure 6.

## VACUUM SYSTEM

### Quadrupole Mass Spectrometer

The quadrupole mass spectrometer, shown in relation to the other components of the vacuum system in Figure 6, consists of an ionizer (or ion source), a mass filter, a detector, and a stainless steel vacuum enclosure.

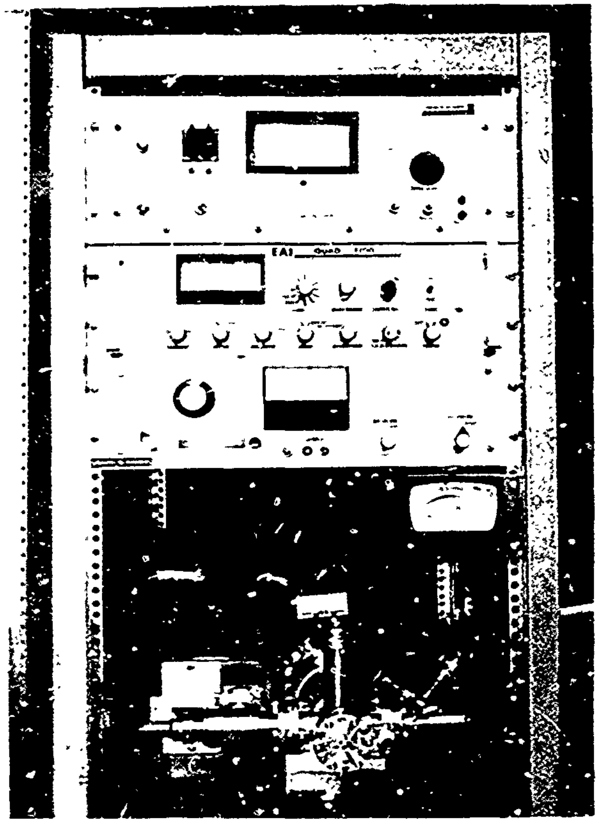

Figure 5. Pulsed Gas Analyzer: Laboratory Model

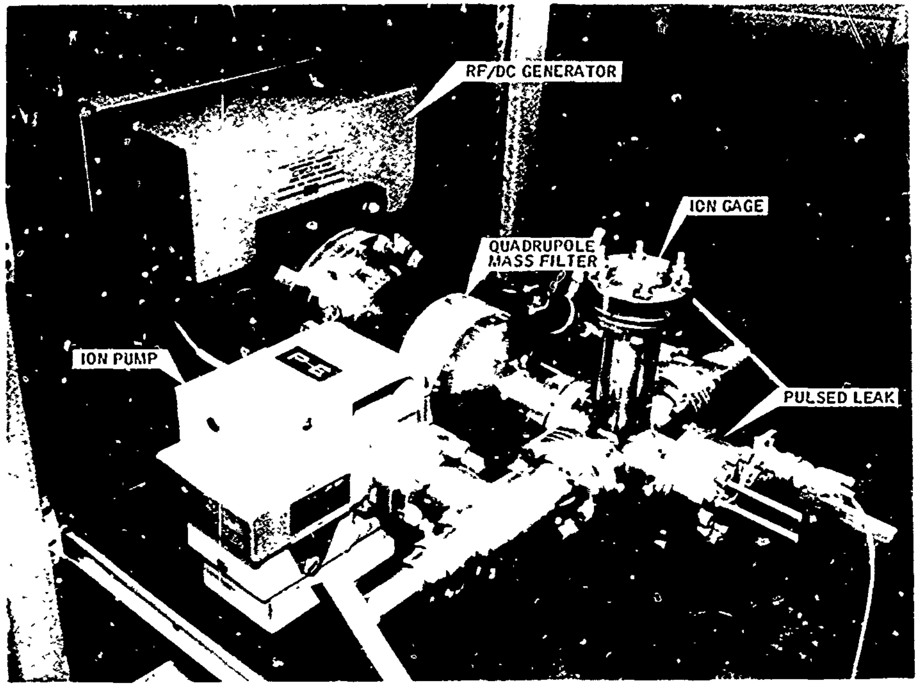

Figure 6. Pulsed Gas Analyzer: Vacuum System

Two basic ionizer configurations have been used with minor modifications. During much of the testing these were driven by external power supplies, and electron and ion energies could be controlled at various levels. The qualitative nature of mass spectra can be changed by using different electron energies in ionizing the gas sample while the resolution of the mass spectra is affected by the ion energy. The first ionizer configuration is shown schematically in Figure 7. This ionizer consists of two filaments with their electron repellers and a Faraday cage. The filaments are series-connected and emit electrons when heated by an electric current. Each filament is electrically common at one end with its electron repeller. Electrons emitted by the filament pass through slits in the electron repeller and enter the Faraday cage through corresponding slits. Molecules of the sample gas admitted by the pulsed leak enter the Faraday cage where they become ionized by the stream of electrons flowing essentially at right angles to the gas plume. The Faraday cage is maintained at a given positive potential with respect to the filament, thus establishing an electron energy level sufficient for the desired degree of ionization. The electron energy is programmed so as to ionize MMH and $NO_2$ but not other atmospheric gases having a higher ionization potential. When detecting the argon isotope during the self-calibration pulse event, the electron energy can be increased sufficiently to ionize argon. The Farady cage is maintained at a low positive voltage (usually about 8 volts) with respect to the quadrupole inlet aperture, and the resultant electric field serves to drive the positive ions from the cage through the grounded inlet aperture. A potential of 8 ev establishes a suitable velocity for the ions traversing the quadrupole mass filter so that the desired degree of mass resolution is obtained in the filter.

The second ionizer configuration is shown schematically in Figure 8. This ionizer has an open cylindrical grid structure with surrounding filament, an extractor electrode, and three focusing lenses (the latter two being cylindrical). The filament consists of two parallel-connected, coiled tungsten legs having a surface area for electron emission over seven times that of the first ionizer. Electrons from the filament enter the ionizing region radially and at right angles to the molecule plume from the pulsed leak. Positive ions are extracted on the pulsed leak/quadrupole axis and focused by the three lenses for entry into the quadrupole. A relatively high negative potential on one of the lenses serves as a barrier to prevent electron flow into the quadrupole.

The ionizing regions of the two ion sources are about equal in volume, but the length of the second configuration is nearly six times that of the first. Its maximum electron emission rating is 50 milliamperes compared to 3 milliamperes for the first configuration. Theoretically, these emissions are obtained at 2325°K and 2400°K filament temperatures and 2.3 and 22.1 watts filament power, respectively. The second ion source has greater electron flux and ionizing capability, but at the expense of higher filament power and more complexity in ion focusing.

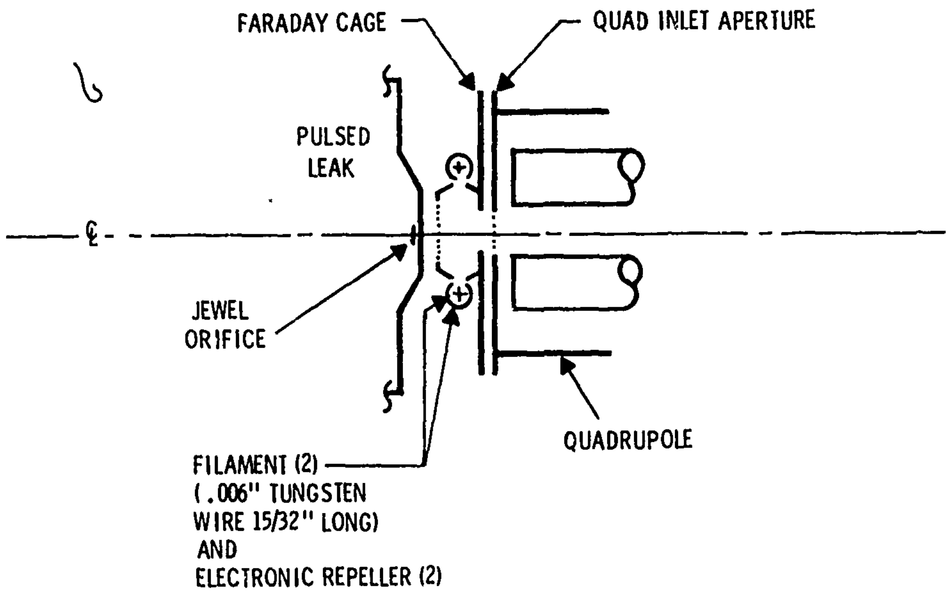

Figure 7. Ion Source No. 1: PGA Laboratory Model

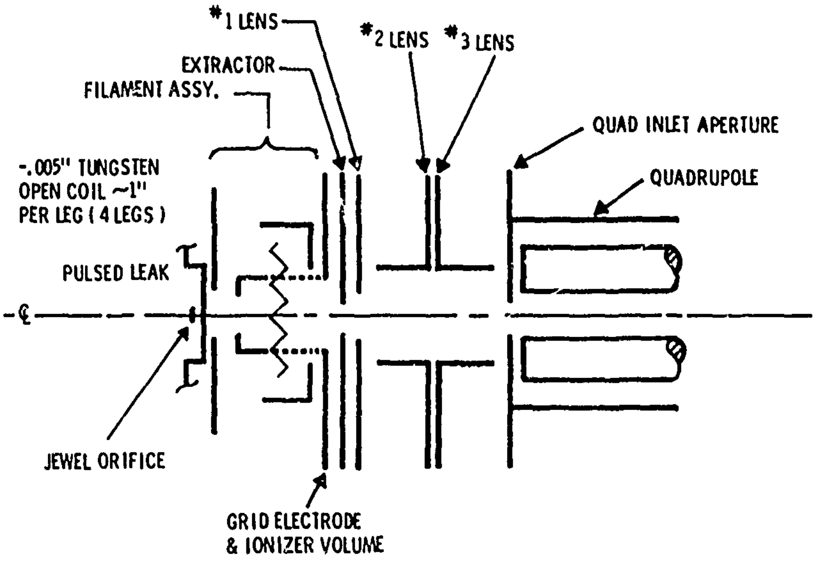

Figure 8. Ion Source No. 2: PGA Laboratory Model

Two minor modifications were made to the second ionizer configuration by which an axial and a radial shield were added adjacent to the filament; in addition, the filament and its shielding were made electrically common and isolated electrically from other elements of the ion source. This was done to remove the electrical potential across the filament support insulators, minimizing surface leakage and emission loss.

The quadrupole mass filter is a device which allows only ions of a given mass number, or atomic mass unit (amu), to pass through it and to reach an ion current detector. The quadrupole mass filter is shown schematically in Figure 9. Ions from the ionizer enter the quadrupole through an electrically grounded aperture. These ions are acted upon by electric fields established by two pairs of rod electrodes. Opposite rod pairs apply dc and superimposed RF fields of opposite polarity and phase so that ions traversing the axis of the rod pairs assume oscillatory trajectories. Careful control of the dc/RF voltages causes ions of a specific mass to pass the entire length of the quadrupole, while the oscillations of ions of all other masses increase in amplitude until collision occurs with a rod electrode and they are removed from the ion beam. The quadrupole mass filter is based on the equations of motion of charged particles (positive ions in this case) responding to the force imposed by simultaneously applied RF and dc fields. Heavy ions are influenced by the dc field, while lighter ions respond to the RF field. These field strengths are increased in sweep fashion when taking a mass spectrum, meanwhile keeping the dc/RF amplitude ratio constant. When detecting single-mass peaks, the rod pairs are excited at given dc/RF voltage levels which allow the ion species of interest to pass through the filter. No axial velocity is imparted to the ions in these fields and they traverse the length of the quadrupole at the velocity at which they leave the ionizer. The length of the quadrupole rods (about 5 inches), the RF frequency (2.5 mHz), and the ion energy (about 8 volts) interrelate so that the ions traversing the filter are subject to sufficient oscillatory periods to obtain the desired degree of separation of ion masses. As this separation capability (resolution) is enhanced, fewer ions traverse the quadrupole to impinge on the detector, with a resultant decrease in ion current at the detector. Thus, resolution and sensitivity are tradeoffs in the operation of the mass filter. By noting the magnitude of the detected ion current at the time of application of a given dc/RF voltage amplitude to the quadrupole, it is possible to determine both ion identity and ion abundance (i.e., qualitative and quantitative analysis).

Ions which traverse the entire length of the quadrupole mass filter impinge on the detector and generate an electrical signal proportional to the population of a given species in the atmospheric mixture. The detector operates in two modes: (1) as a Faraday cup without ion current amplification, and (2) as a secondary emission multiplier (SEM) in which the detected signal is amplified through the cascading of electron populations in successive collisions with electron-emitting surfaces (dynodes). Changing the operation from Faraday cup to SEM is done by electrical switching; SEM operation was

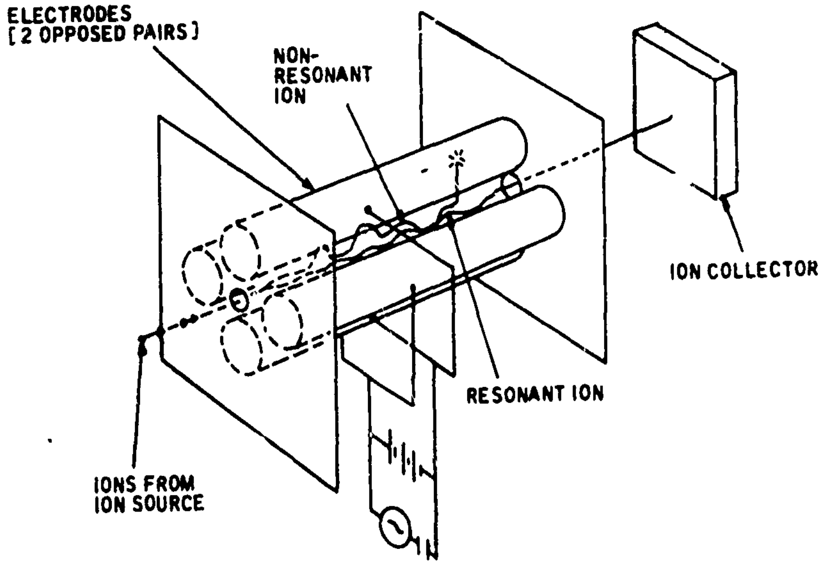

Figure 9. Schematic of Quadrupole Mass Filter

done almost exclusively in the test program. The SEM detector is a 14-stage, venetian-blind type having a gain of about $10^5$. Positive ions traversing the quadrupole mass filter strike the first dynode, causing secondary electrons to be emitted. These secondary electrons are accelerated by an applied electric field and impinge upon the second dynode, causing additional electron emission. This process is repeated through the 14 stages, resulting in a greatly increased electron current. The electrical gain of the SEM increases as the applied voltage is increased. At full gain a potential of 3000 volts is applied across the 14 stages.

The vacuum enclosure of the quadrupole mass spectrometer is a bottle-shaped, stainless steel envelope having a 6-inch-diameter flange at the signal output end and a 2-3/4-inch-diameter flange on the gas inlet end. Electrical connections for signal, quadrupole excitation, and ion source excitation are made using vacuum feed-throughs in the 6-inch flange. The 2-3/4-inch-diameter flange is bolted to a modified cross fitting opposite the pulsed leak. The pulsed leak admits a plume of sample gas directly into the ion source in this arrangement. Two other branches of the cross fitting attach by copper-gasketed flanges to the roughing pump line and the ion pump line. Each of these can be sealed off by all-metal valves. A fifth leg of the modified cross contained an ion gauge during a portion of the test program.

## Ion Pump

The ion pump used for the PGA laboratory model is a commercially available, differential ion type having 11-liter-per-second pumping capacity. This pump uses a magnetic rather than an electric field and was chosen to expedite the test program because it provided ample pumping capacity and was immediately available. The ion pump removes the sample gas from the vacuum enclosure and any leakage. Typically, the system is maintained at a pressure of $10^{-8}$ torr or less when not pulsing. Pressure increases momentarily, into the $10^{-6}$ torr range, upon the pulsing of sample gas into the system. The ion pump is not a pump in the usual sense since it traps gas within its walls rather than expelling it. The pump operates entirely from electrical power and does not require any working fluid or refrigerant. It also serves as its own vacuum gauge since the current drawn by the pump is directly proportional to system pressure. Operating life is in excess of 32,000 hours at $10^{-6}$ torr pressure.

The differential ion pump is shown schematically in Figure 10. The principal pump elements are a pair of cathodes; an intervening, cellular anode; and a magnet in the classical Penning arrangement together with pump housing and electronic controls. The uniqueness of the differential ion pump is the use of dissimilar cathode materials, one of tantalum and one of titanium. Tantalum has a higher sputter rate than titanium, giving rise to deposition of a thin film of tantalum at peripheral areas of the titanium cathode. This deposition minimizes re-emission of gases after trapping, making it possible to pump inert gases rapidly and stably. In the Penning electrode arrangement, a magnetic field at right angles to the electrodes causes electrons leaving the cathodes for the anode to travel helical paths, thereby providing much longer travel distance than in direct flight and increasing the probability for ionizing the gas molecules present. Positive ions are formed in collisions between gas molecules and electrons with subsequent attraction of the ions to the cathodes. At ion impact at the cathodes there can be:

- Sputtering by ejection of cathode atoms
- Secondary electron emission from the cathode (thereby contributing to the pumping)
- Penetration of the cathode and burial
- Acquisition of an electron and reflection in the gas phase
- Re-emission of previously absorbed gas

The differential ion pump lessens this last process by using dissimilar cathode materials. As a consequence, argon and other inert gases are more effectively trapped, and pumping speeds for these gases are improved.

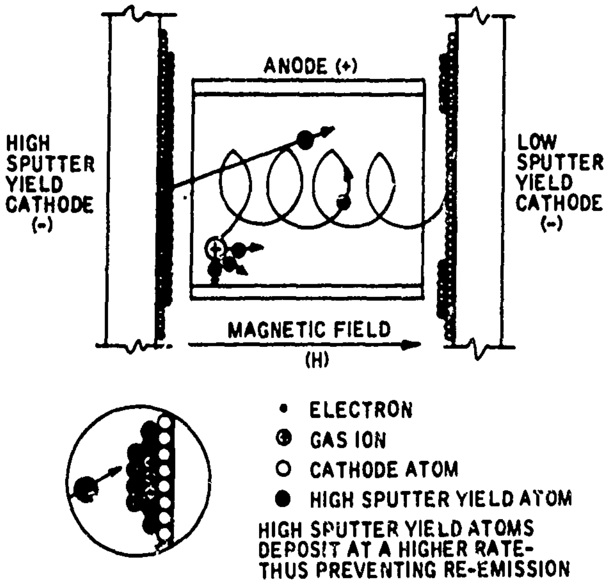

Figure 10. Differential Ion Pump Schematic

## Pulsed Leak

The pulsed leak is a normally closed, miniature valve which can be opened briefly by application of a voltage pulse to admit a gas sample to the ionizing region of the quadrupole mass spectrometer. When closed, its leak rate is small enough to maintain a high order of vacuum (about $10^{-8}$ torr) in the mass spectrometer. Sealing quality is about the sensitivity level of a helium leak detector. When a voltage pulse is applied, a small amount of sample gas passes through the leak directly from the atmosphere to the ionizing region of the ion source. Depending on the duration and wave shape of the voltage pulse, gas samples in the range of $10^{-10}$ to $10^{-7}$ moles are admitted at each pulse event. The pulsed leak's flow rate is determined by pulsing gas into a known volume and measuring pressure differential brought about by pulsing. Since sample flow is in the viscous flow regime, it is believed that fractionating of the sample according to the molecular weight of the constituents in the sample gas does not occur.

## Roughing Pump System

The roughing pump system consists of a 21-liter-per-minute mechanical vacuum pump, a cryogenic trap, a metallic adsorbent trap, a thermocouple gauge, an all-metal valve, and connecting tubulation. The roughing pump system is used to establish the initial vacuum in the mass spectrometer vacuum enclosure. When the system pressure has been lowered to 5 microns ($5 \times 10^{-3}$ torr) or less by the roughing pump, the ion pump takes over and further lowers the pressure to the $10^{-6}$ to $10^{-8}$ torr range. When the initial rough vacuum has been established, the roughing pump system is closed off from the remainder of the system by the all-metal valve. The roughing pump system is used infrequently only at those times when the entire system has been let up to atmospheric pressure for repair or modification.

### Ion Gauge

The PGA laboratory model was initially operated with an ion gauge. This was installed in the vertical branch of the modified cross (reference Figure 6). The gauge was later removed to minimize outgassing in the mass spectrometer vacuum space. After that time, system pressure was determined solely by the vacuum gauge provided with the ion pump.

The ion gauge, of the Bayard-Alpert type, consists of a cylindrical grid, a collector wire along the grid axis, and a spiral filament parallel to the collector wire but outside of the cylindrical grid. Electrons are emitted from the filament at a controlled rate and are attracted to the grid space by the electric field existing between the filament and grid. The electrons have sufficient energy to ionize the gas present in the grid space. The resultant ions are then attracted to the collector wire and collected as an ion current. This current is directly proportional to the density of molecules in the gauge space, hence to the pressure. The ion current is measured in an external electrometer circuit and used to drive a meter and/or recorder to give pressure readout(s).

## ELECTRONICS SYSTEM

### Quadrupole Control

The quadrupole control is a rack-mounted unit together with a dc/RF voltage generator unit mounted on the 6-inch flange of the quadrupole mass spectrometer. The rack-mounted unit, shown as the second unit from the top in Figure 5, contains the ionizer control, dc/RF generator control, detector control, and recorder control. The dc/RF voltage generator is seen at the top of Figure 6.

The quadrupole control establishes and maintains operating conditions for the ionizer, dc/RF generator, and the detector. In addition, the control provides the amu correlation signal (horizontal sweep) to the recording instrumentation. The quadrupole control consists of a control panel and chassis, four electronic modules, a test point module, and cabling connecting to the quadrupole mass filter. The controls seen on the panel in Figure 5 include:

- AMU/emission meter
- Meter switch
- Filament switch
- Mass range switch
- Center mass switch
- Resolution control

- Emission control
- Scan speed switch
- Start/End scan switch
- SEM voltage control
- Mode switch
- Power switch

The control unit provides for the following performance features:

- Mass Range: 1 to 300 amu
- Resolution: Unit resolution (or $M/\Delta M \geq 2M$)[2]
- Scan Rates: 0.1, 0.3, 1, 10, 30, 60, 150, 300, 450, 600, 900 seconds per mass range
- Emission: Variable: 100µ A to 3mA

The four electronic modules provide the following voltages and data correlation signals for operation of the quadrupole mass filter:

- Filament supply and electron emission
- Electron energy
- Ion energy
- Quadrupole drive ramp
- SEM excitation

The first three of the above functions relate to operation of the ionizer. For much of the testing these were provided, not by the control unit, but by external power supplies. This was to provide for greater testing versatility in that electron and ion energy levels could be controlled.

One of the electronic modules generates a 0- to 10-volt sweep, or quadrupole drive ramp, which drives the dc/RF voltage generator. This sweep voltage provides the means for obtaining a continuous mass spectrum of the entire mass range of the quadrupole mass spectrometer. To do this the dc/RF amplitudes are continuously changed in linear fashion while maintaining their ratio constant. As this sweep occurs, progressively larger ion mass numbers are made to be resonant in the quadrupole mass filter and a continuous mass spectrum is produced. The 0- to 10-volt sweep can be manipulated by the panel controls so that any portion of the sweep may be used to produce any mass scan range in the range of instrument. The range of the mass spectrum can be narrowed or broadened, or the center of the mass spectrum can be reached more or less rapidly in the sweep so as to position the spectrum horizontally in an oscilloscope display, or a single mass number

---

[2] M is the mass (amu) number and $\Delta M$ is the peak width measured at half peak height

may be continuously monitored, or an external program can be introduced by which any number of mass numbers may be monitored individually. This latter mode of operation was used extensively in the test program so that amu 45 and amu 46 could be individually monitored to obtain an MMH and $NO_2$ signal. The 0- to 10-volt sweep can be made to occur at various rates by the scan rate control so that a mass spectrum may be made as quickly as 0.1 second or as slowly as 900 seconds. In most of the testing the scan rates were 60 seconds and slower. This was so that several pulses of sample gas could be made while sweeping across one mass number when the pulses were at a rate of about 0.5 to 1 per second.

Another of the electronic modules contains a dc-to-dc converter that generates up to 3000 volts for excitation of the secondary emission multiplier (SEM) detector. This voltage is variable by potentiometer adjustment on the control panel. Precautions are taken in shielding because of the magnitude of this voltage and the need to minimize circuit noise.

The dc/RF voltage generator is driven at the command of the 0- to 10-sweep, or ramp, voltage and provides the voltage excitation for the rod pairs of the quadrupole mass filter. The RF generator provides a linear RF ramp from 0 to 2400 volts (peak to peak) at a frequency of 2.5 mHz. The RF voltage is fed to diagonally opposed rod pairs at a 180-degree phase angle. The RF generator is closely located to the quadrupole mass filter to reduce power requirements and to allow solid-state components to be used. The dc generator provides the plus and minus ramp voltages - each fed to one of the two pairs of diagonally opposed quadrupole rods. The magnitude of the dc ramps is approximately 200 volts. The voltage does not rise linearly but in three linear steps so that three RF-to-dc voltage ratios are actually used in obtaining the full 0 to 300 amu range of the spectrometer. The ratio of the RF-to-dc voltage is approximately 6 to 1.

The RF voltage ramp is generated by the Q multiplier technique. The quadrupole rods act as capacitive reactances and dissipate little power because of their high Q; therefore, an inductor of the proper value is used to series resonate the capacitive load. The resonant frequency is 2.5 mHz, and the equivalent series resistance at resonance is a function of the Q of the air core inductor.

The RF and dc voltage ramps are synchronized by detecting the RF signal and parallel feeding both dc rod drive amplifiers and the RF control operational amplifier. A ratio control varies the slope of the dc ramp with respect to the RF ramp to obtain the three ratios needed in obtaining a 0- to 300-amu mass spectrum. A relatively small change in dc-to-RF voltage ratio has a significant effect on the spectrum scan and is used as the basis for the resolution control of the quadrupole mass spectrometer. In effect, the resolution control shifts the start point of the dc ramps with respect to the RF.

## MMH-$NO_2$/Control-Display Unit

In the latter part of the test program, an MMH-$NO_2$/Control-Display (MN/CD) Unit was designed and fabricated to allow automatic monitoring of mass numbers 45 and 46. In addition, provision was made to monitor argon 38, an isotope normally present in the atmosphere, as a standardization method. Pulse drive circuits, ionizer voltages, and readout meters are also provided. The MN/CD unit is shown in Figure 11. A block diagram is shown in Figure 12.

The MN/CD Unit has several functions:

- Programs the pulsed leak openings at a prescribed rate and provides its driving voltage pulse
- Programs the dc-RF voltages on the quadrupole rods
- Programs the electron energy within the ion source
- Provides meter-type and recorder jack readouts of MMH and $NO_2$ concentrations

The control section of the MN/CD unit has three subsections:

- Voltage generators for quadrupole mass filter operation
- Gate control generators to control the display functions
- System sequencing

Given voltages are established for exciting the quadrupole mass filter for monitoring amu 45 (MMH), amu 46 ($NO_2$), and amu 38 (argon$^{38}$). Voltages are also applied to establish the proper electron energy for ionizing MMH and $NO_2$, and for argon 38. Finally, a voltage pulse train is applied to the pulsed leak having a frequency of about 0.5 Hz with pulse width of about two milliseconds. Fifteen logic states are used in the sequencing of the MN/CD unit. Amu 45 and amu 46 are monitored alternately by the progression of 14 of these states, while the fifteenth is used to monitor amu 38, the argon isotope used for self-calibration of the system. A pulse peak detector circuit is opened coincidentally with the gas pulsing event, and the proper gate of three sample-and-hold gates is opened for about two milliseconds immediately after the pulsing.

The sequence control consists of 14 dual-in-line 5400 series TTL logic elements. The sequence control is mechanized around a module 15 counter. Immediately after turning on system power, 15 pulse events with control settings for amu 38 are taken to standardize the system. On all subsequent passes through the pulse counter the first pulse updates the amu 38 reading, even-numbered pulses 2 through 14 monitor amu 45, and odd-numbered pulses 3 through 15 monitor amu 46.

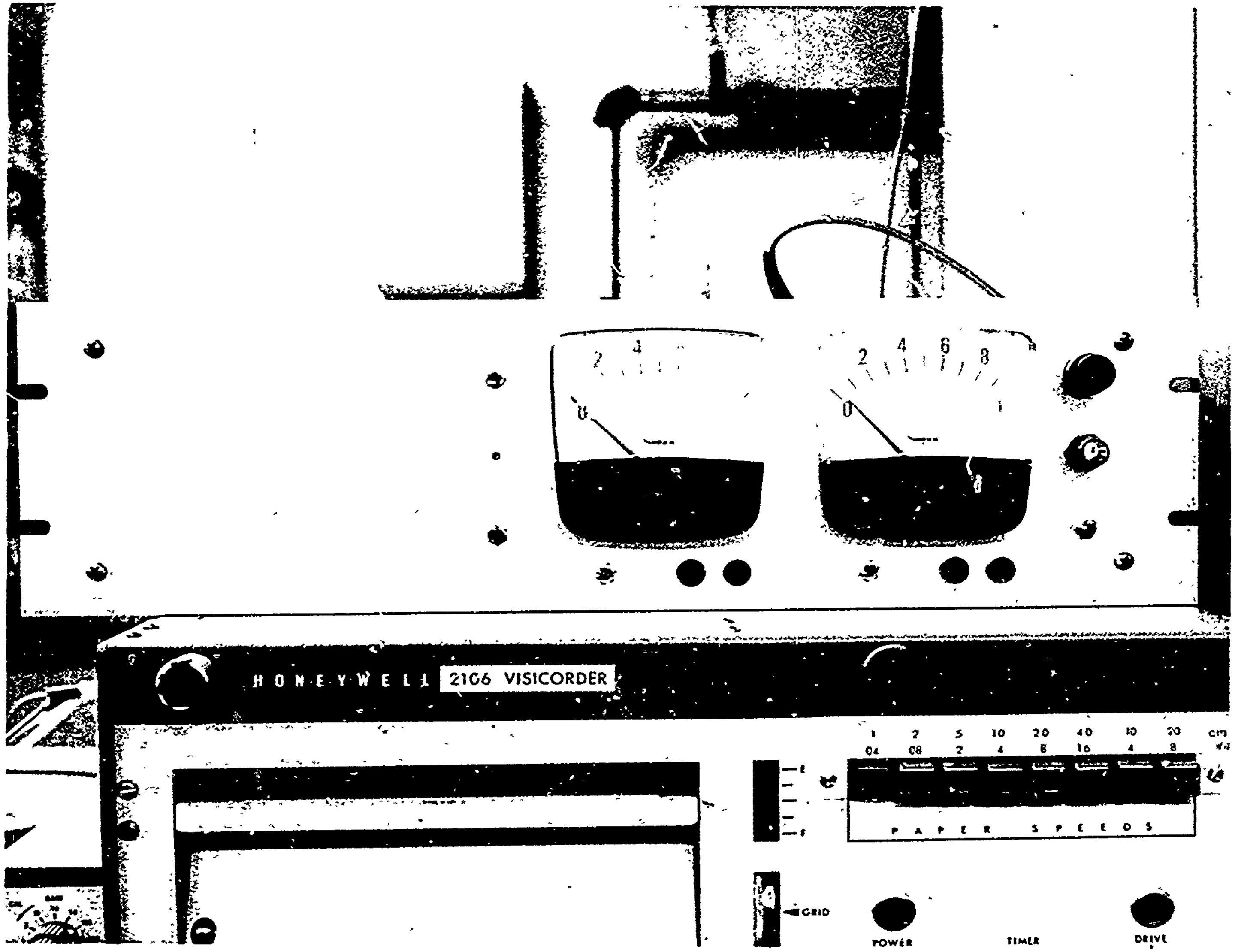

Figure 11. MMH/$NO_2$ Control Display Unit

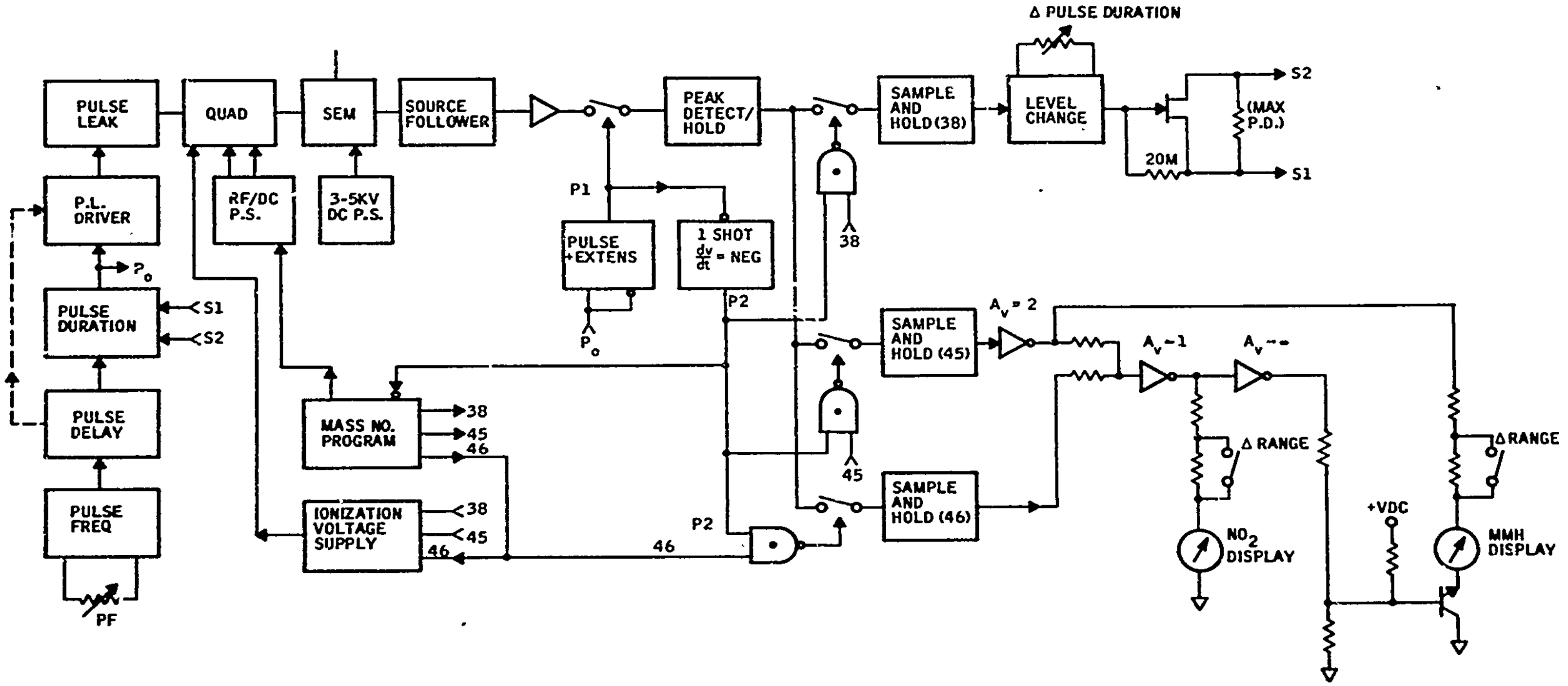

Figure 12. Block Diagram of MMH/$NO_2$ Control Display Unit

The display section of the MN/CD unit contains an amplifier, pulse peak detector, three sample-and-hold circuits, and signal processing and readout circuitry.

The amplifier circuitry of the MN/CD unit consists of a source follower, preamplifier, and a variable gain amplifier. The input of the source follower is connected to the SEM detector. The source follower provides an impedance match with the SEM detector. The preamplifier and variable gain amplifier amplify the source follower output voltage. The gain of the amplifier is varied by manual switches in the present design, but automatic gain control can be provided in response to the argon isotope signal level.

The pulse peak detector stores the pulse peak amplitude momentarily when a given mass number is monitored until a series gate to one of the three sample-and-hold circuits is opened. These sample-and-hold circuits store voltages proportional to the detected signals at amu 45, 46, and 38. Each sample-and-hold circuit is scaled at a 20 percent update level with respect to the pulse peak detector. This means that 20 percent of the voltage difference existing between the peak detector capacitor and the sample-and-hold capacitor is transferred (in either direction) at each pulse event. This update fraction was chosen because of the requirement to show initial readout response in 10 seconds and to reach 90 percent of the steady-state readout value in 1 minute. Actually, when pulsing at 0.5 cycle per second, signal response to MMH or $NO_2$ presence would occur in 6 seconds, and 90 percent response would occur in 43 seconds.

The signal processing and readout circuitry is predicated on the use of the amu 45 peak for MMH readout and the amu 46 peak for $NO_2$ readout. MMH has an amu 45 peak and an accompanying amu 46 peak twice its amplitude. $NO_2$ has no amu 45 peak, but does have an amu 46 peak. Advantage is taken of this situation in constructing the readout logic for MMH and $NO_2$. No MMH reading will occur if twice an amu 45 peak is greater than an accompanying amu 46 peak. No $NO_2$ reading will occur unless the amu 46 peak is greater than twice the amu 45 peak.

### Ion Pump Control

The ion pump control is contained in a rack-mounted chassis seen at the top of Figure 5. The ion pump control is essentially a high-voltage, current-limited power supply. When operating, its output is about 5 kilovolts.

Within the ion pump control chassis there is a leakage, inductance type power transformer; an encapsulated full-wave diode rectifier bridge; and capacitors and resistors forming a part of the power output circuit. In addition, there are components used with the metering and test voltage output circuits. The control is supplied with circuit breakers to protect the unit itself and the ion pump from excessive current flow.

The ion pump control is operated using the controls on its front panel which include:

- Range selector
- Meter
- Main circuit breaker
- Mode switch
- Indicator lights
- Recorder output and adjust

The range selector provides for ion current readout in five ranges from 20 μamps to 200 m amps. It also provides for direct pressure readout in the range of $10^{-8}$ to $10^{-5}$ torr. A selector position is also provided for reading output voltage to the ion pump up to 5 kilovolts. As implied in the foregoing, pump pressure and pump current are accurately related. Throughout most of the test program the ion pump current was used to monitor the pressure of the entire PGA vacuum envelope.

## Ion Gauge Control

The ion gauge control is the chassis seen as the lowest of the three pictured in Figure 5. As noted previously the ion gauge was used but a short time during the test program because an alternate system pressure readout was available in the ion pump and because it was desirable to remove any elements in the vacuum envelope subject to outgassing.

The ion gauge control provides an emission-regulated electron current and a meter readout of pressure in the range of $1 \times 10^{-3}$ torr to less than $1 \times 10^{-10}$ torr. The control also provides for degassing of the grid of the gauge by $I^2 R$ heating and for overpressure trip-out.

# SECTION VI

## DESCRIPTION OF TEST METHOD FOR FEASIBILITY DEMONSTRATION

The experimental phase of the program was designed to show (1) verification of sensitivity of the PGA laboratory model to 0.2 ppm MMH and 5.0 ppm $NO_2$, (2) response over range 0 to 100 and 0 to 500 ppm MMH and $NO_2$, (3) response of the instrument to possible interfering compounds, and (4) operation at extremes of temperature and humidity. A vapor-dilution apparatus was constructed for use in the sensitivity and interference tests, and an insulated enclosure for the quadrupole and accessories was used for the temperature tests.

The dilution apparatus as depicted in Figure 13 consisted of a mixing manifold fed by dilution air, saturated vapors of MMH or 100 percent $NO_2$ and interference vapors. An aliquot of this mixture was passed through the inlet system where it was pulsed into the mass spectrometer. The remainder of the mixture was exhausted into a fume hood. Figure 14 shows the test configuration for the temperature tests. The insulated box contained the mass spectrometer, the pulsed leak, and the ion pump. Temperature-conditioned air was passed to and from the enclosure by means of four-inch-diameter hoses connected to a temperature chamber. Dry ice was used to produce cold air while electric heaters provided hot air. Temperatures were monitored with thermocouples placed in the air and on the case of the mass spectrometer. Figure 15 shows the dilution apparatus including mixing manifold. Also shown is the temperature enclosure.

MMH concentrations were generated by passing nitrogen gas at a known flow rate through a flask containing MMH. Nitrogen was used to avoid loss of MMH by oxidation from atmospheric oxygen. The saturated vapor was then mixed with charcoal-filtered air from a compressed air line to provide the desired concentration. Table IV shows examples of flow rates used and the resulting concentrations.

Table IV. MMH Concentrations and Flow Rates

| Flow Rate: Dilution Air (LPM) | Saturated MMH in Nitrogen (cc/min) | Resulting MMH Concentration (ppm) |
|---|---|---|
| 10 | 16.0 | 104.0 |
| 10 | 10.0 | 65.0 |
| 10 | 5.0 | 32.5 |
| 10 | 1.0 | 6.5 |
| 10 | 0.2 | 1.3 |
| 35 | 0.2 | 0.37 |
| 35 | 0.1 | 0.19 |

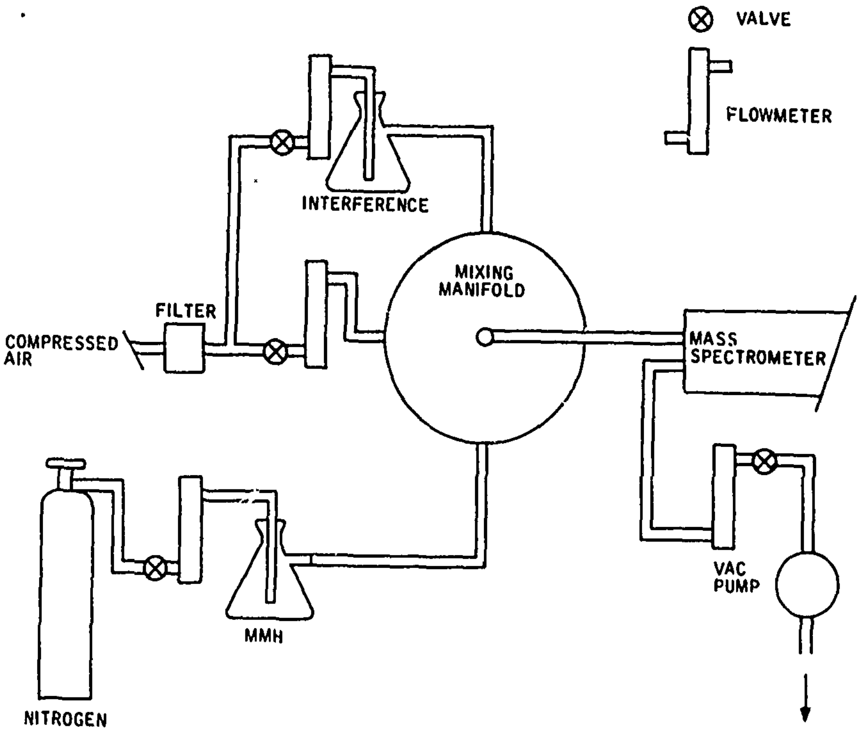

Figure 13. Schematic of Dilution Apparatus

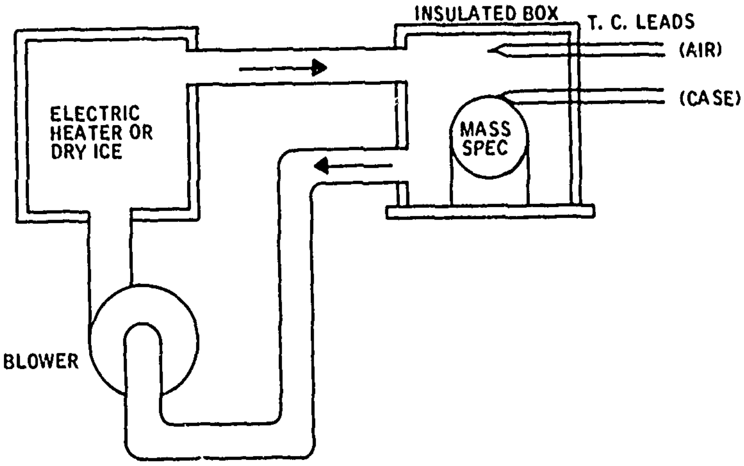

Figure 14. Temperature Test Configuration

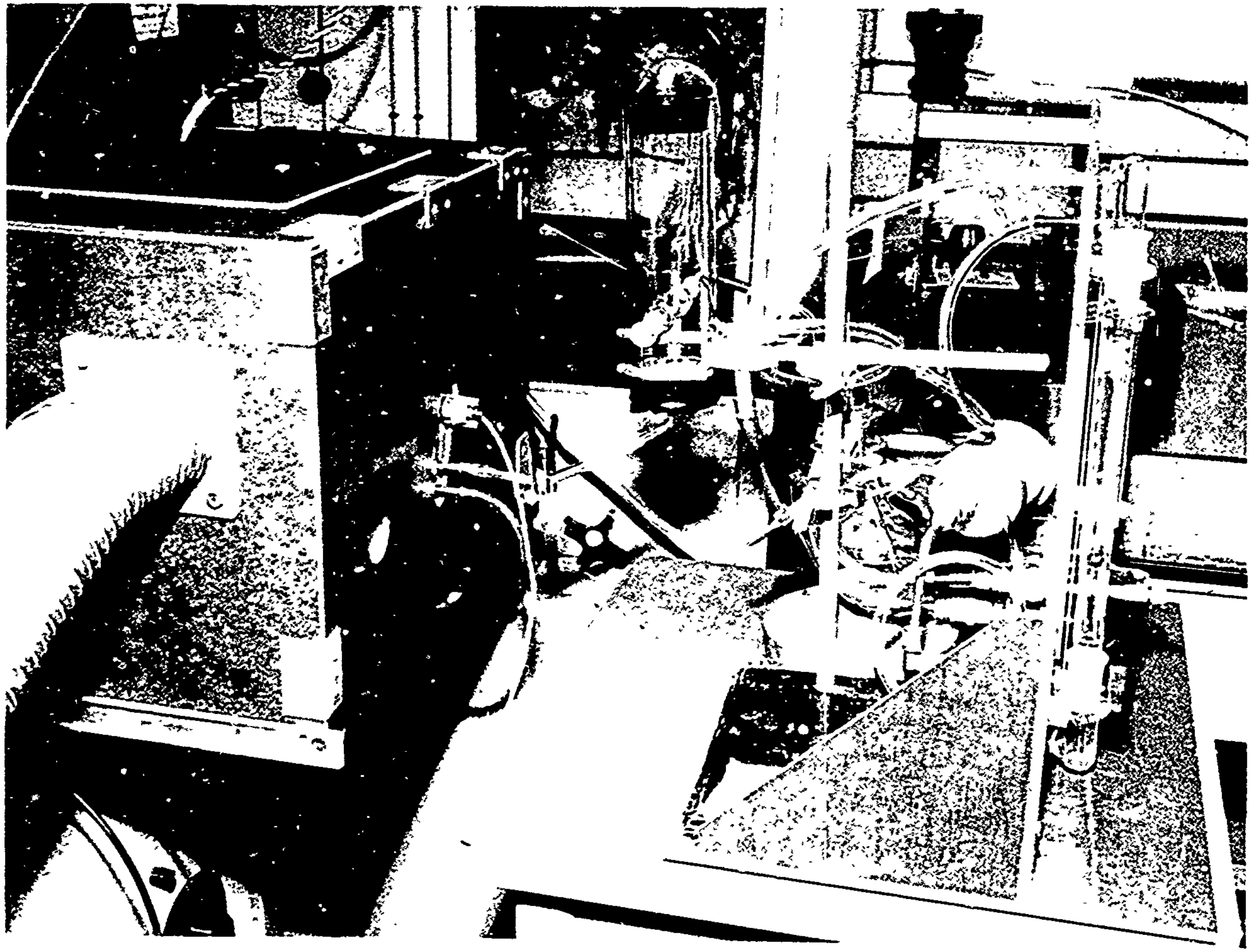

Figure 15. Dilution Apparatus and Temperature Enclosure

$NO_2$ concentrations were generated in two ways.[3] During the interference testing $NO_2$ gas (99.5 percent pure) from a cylinder was metered through a flowmeter into the mixing manifold in a manner similar to that used for MMH. Table V gives the flow rates used to achieve the desired $NO_2$ concentration.

Table V. $NO_2$ Concentrations and Flow Rates (Dynamic)

| Flow Rate: Dilution Air (LPM) | Flow Rate: $NO_2$ (cc/min) | Resulting NO2 Concentration (PPM) |
|---|---|---|
| 10 | 5 | 500 |
| 10 | 1 | 100 |
| 10 | 0.5 | 50 |
| 10 | 0.2 | 20 |
| 35 | 0.5 | 14 |
| 35 | 0.2 | 5.7 |

For sensitivity tests, measured volumes of $NO_2$ gas were injected into a 5-liter polyethylene container to provide a known concentration. Table VI shows the volumes needed to give a known concentration of $NO_2$.

Table VI. $NO_2$ Concentrations and Dilutions (Static)

| Air Volume (liters) | $NO_2$ Volume (cc) | Resulting $NO_2$ Concentration (PPM) |
|---|---|---|
| 5 | 2.5 | 500 |
| 5 | 1.25 | 250 |
| 5 | 0.5 | 100 |
| 5 | 0.25 | 50 |
| 5 | 0.1 | 20 |
| 5 | 0.05 | 10 |
| 5 | 0.037 | 7.5 |
| 5 | 0.025 | 5 |

For each sampling, two 5-liter containers were prepared identically and connected in series. At a sampling rate of 0.5 LPM through the PGA inlet system, this arrangement provided a very slow exponential decay of concentration, allowing several minutes of sampling without significant concentration reduction. Relative humidities of less than 5 percent and greater than 95 percent were provided by passing the dilution air through a silica gel desiccator or a water bubbler prior to the mixing manifold, as shown in Figure 16. For the $NO_2$ humidity tests, the 5-liter containers were flushed with desiccated air or water-saturated air prior to adding the $NO_2$ gas. Interfering vapors and gases were introduced through an additional inlet in the mixing manifold.

---

[3] Concentration values of $NO_2$ in this report are given on the basis of dissociated $N_2O_4$. These values should be multiplied by the factor 1.7 to take into account the monomer-dimer equilibrium prior to dilution.

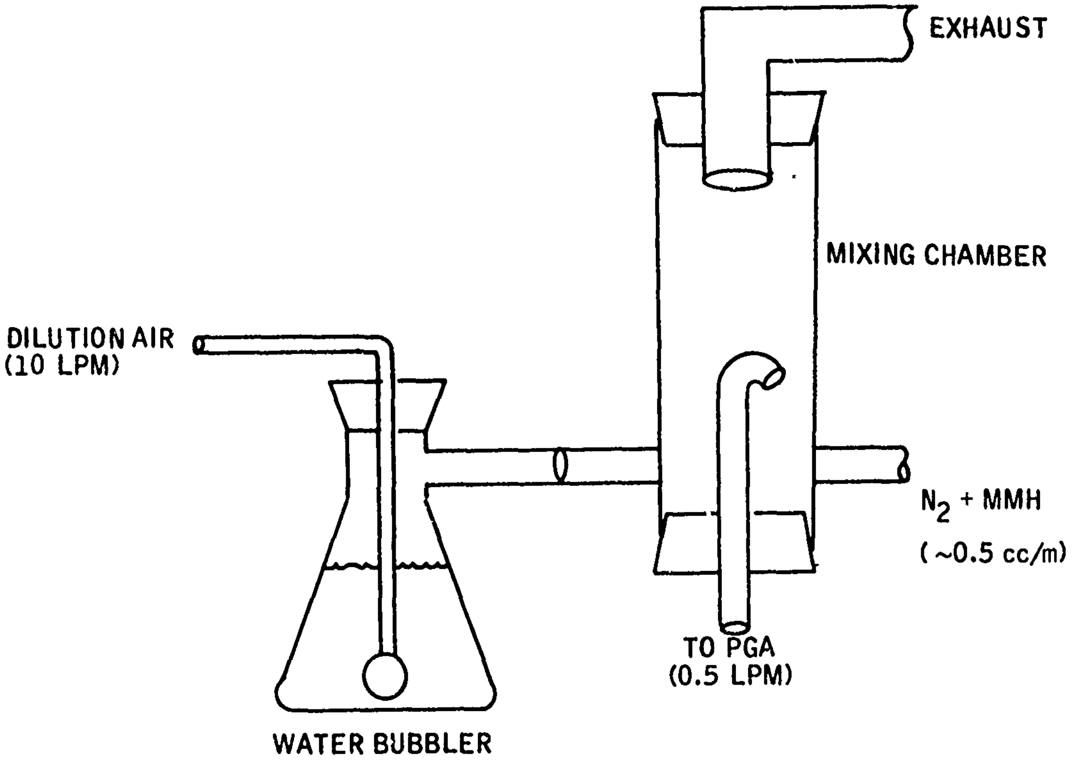

Figure 16. Dilution Apparatus as Used for High-Humidity Testing

Data obtained in the earlier parts of the test program were recorded mainly on a Honeywell visicorder and oscilloscope. The mass scans appear as a series of vertical lines; each line represents a pulse leak opening. The envelope surrounding the lines designates the mass spectrum. Data obtained after the control panel was put into operation was recorded on a strip chart recorder. The recording is, in effect, the envelope of pulses taken at a fixed mass number. Subsequently, a storage oscilloscope was used which provided an effective means of visualizing the development of mass spectra in real time and of providing a means of obtaining photographic records. Examples of each type of data recording are given in Figures 17, 18, and 19.

A list of materials and equipment used in the testing program is given in Table VII.

Table VII. List of Materials and Equipment Used in the Testing Program

| | |
|---|---|
| Chemicals: | |
| Monomethylhydrazine | Eastman Chemical Co., Catalog No. 7009. |
| Nitrogen Dioxide Gas | Matheson Gas Products, Purity at least 99.5% |
| Carbon Monoxide | Matheson Gas Products |
| Methane | Matheson Gas Products |
| Hydrogen | Air Products Company |
| Nitrogen | Air Products Company |
| Acetone | B and A, Electronic Grade |
| Freon 114 B2 | Honeywell stock |
| Ammonia | B and A, CP Grade $NH_4OH$ |
| Acetaldehyde | Matheson Coleman and Bell, No. 2724 |
| Butyl Amine | J. T. Baker, No. D 72 |
| Propyl Amine | J. T. Baker, No. P 389 |
| Diethyl Amine | J. T. Baker, No. 9216 |
| Dipropyl Amine | J. T. Baker, No. K 848 |
| Equipment: | |
| NJE Power Supply | Model RVC 36-5 |
| Harrison Power Supply | Model 6515A |
| Dressen-Barnes Power Supply | Model 3-150L |
| Trygon Power Supply | Model HR40-5B |
| Trygon Power Supply | Model DL40-1 |
| PGA Laboratory Model | |
| Tektronix D13 Dual Beam Storage Oscilloscope | |
| Dual Trace Amplifier | Tektronix 5A18N |
| Timebase Amplifier | Tektronix 5B10N |
| Picoammeter | Keithly model 4145 |
| Voltmeter, dc | Weston model 31 |
| Vacuum Gauge | Hastings model DV6 |
| Laboratory Stimulator | AEL model 104A |
| Thermocouple Potentiometer | Honeywell, Brown Instr. |
| Honeywell 2106 Visicorder and Accudata 112 Amplifier | |
| Honeywell Electronik 19 Strip-chart Recorder | |
| Flowmeter | Fisher & Porter, No. 3F-3/8-25-5/35 |
| Flowmeter | Gilmont, No. 10 |
| Flowmeter | Matheson, No. 610 |
| Flowmeter | Matheson, No. 603 |

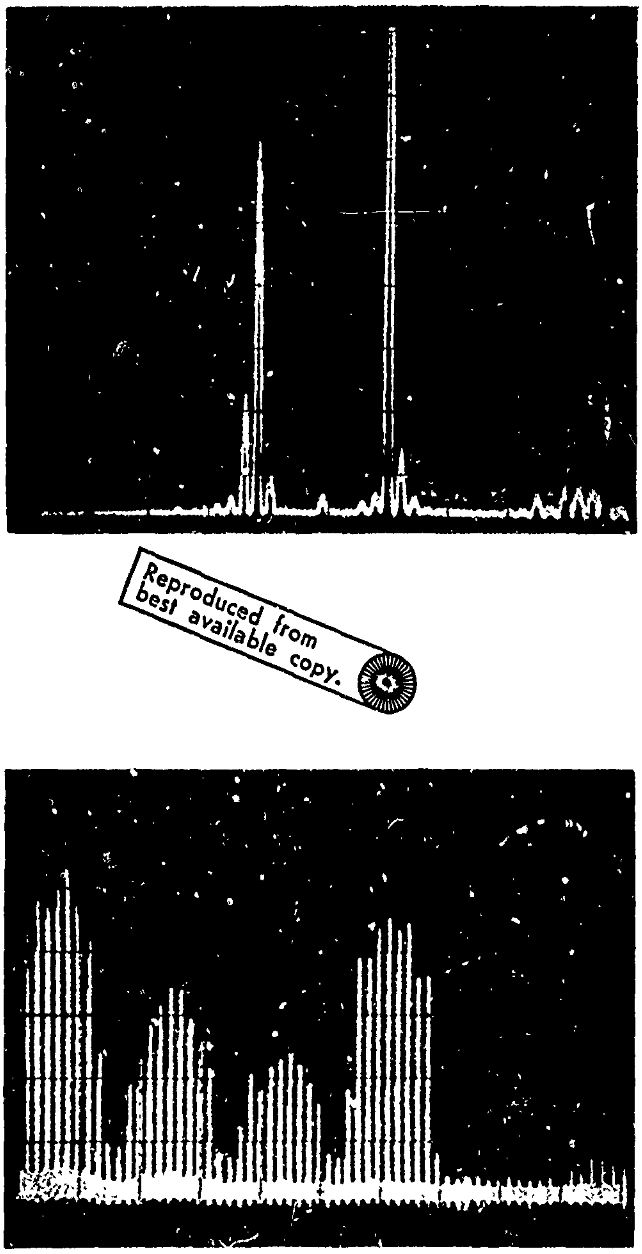

Figure 17. Example of Storage Oscilloscope Photographs of Pulsed and Residual Spectra

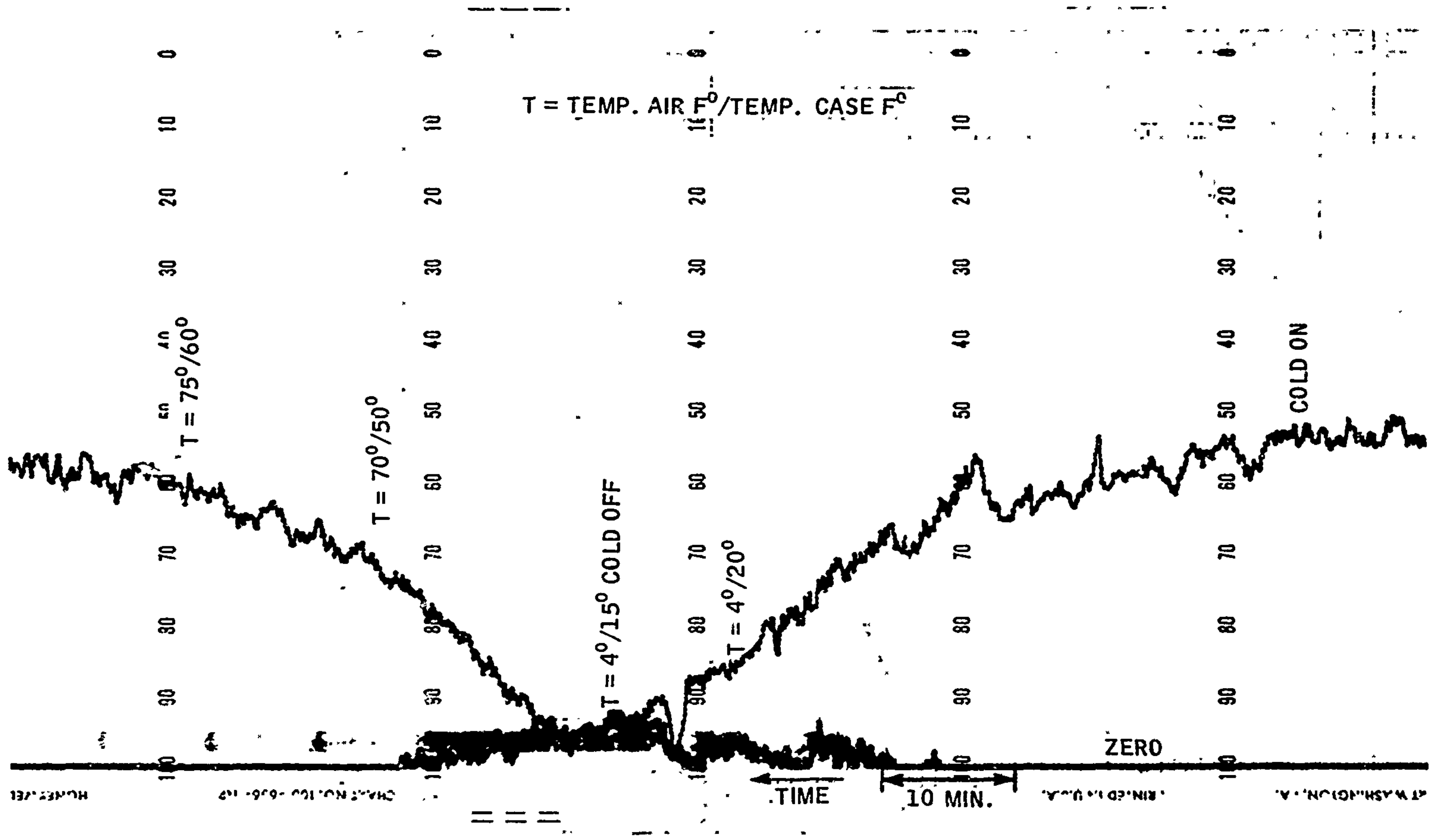

Figure 18. Effect of Temperature on MMH (100 ppm) Response

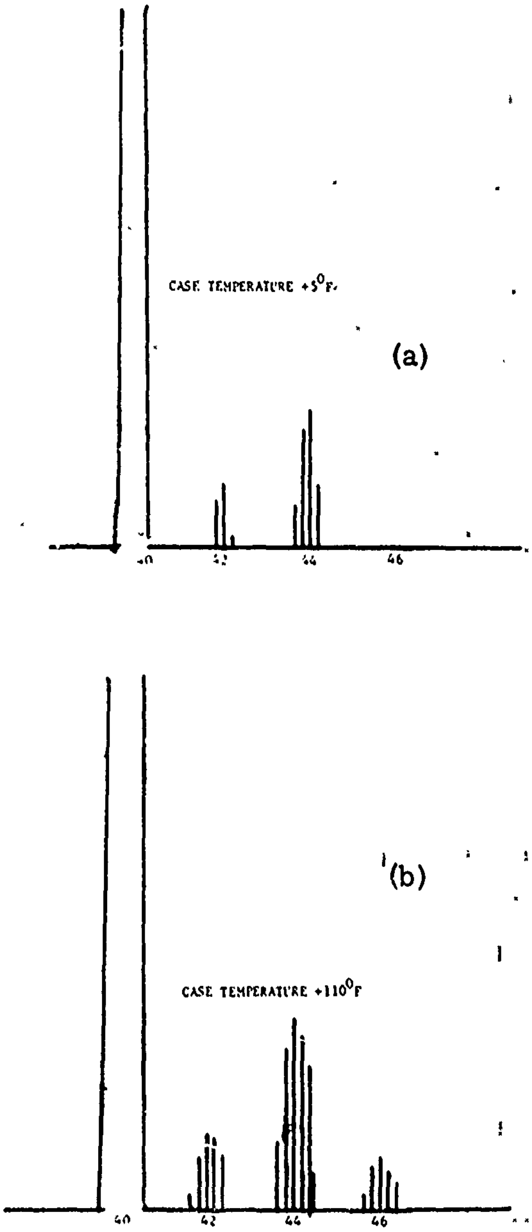

Figure 19. Effect of Temperature on Nitrogen Dioxide Response (Replication)

# SECTION VII

# TEST RESULTS

The program requirements call for the detection and measurement of MMH and $NO_2$ in the atmosphere in the ranges of 0 to 100 ppm and 0 to 500 ppm, respectively. Detectivity and response in these concentration ranges were demonstrated by using the pulsed inlet valve and monitoring mass scans which included amu values 45 and 46. Visicorder recordings of MMH and $NO_2$, and air responses at these levels are shown in Figure 20. Figures 21 and 22 show response curves for MMH and $NO_2$ respectively. Inspection of the spectra from amu 37 to amu 47 (Figure 20) shows that MMH contributes peaks at amu values of 43, 44, 45, and 46, and a small peak at 47. At an ionization energy of 14.8 volts, the value used in taking these data, fragmentation of MMH is kept to a minimum. The parent ion peak (46) and parent ion minus one hydrogen peak (45) are the two major peaks present. The ratio of 46 amplitude to 45 remains essentially constant over the concentration range of interest as indicated in Figure 21. The small peak at amu 47 is most likely due to a rearrangement reaction in which the parent ion attaches a proton. The small peak at amu 45 in the air scan is due to impurities in the system which were subsequently eliminated.

Table VIII is the testing summary for MMH and contaminants. MMH at 100 ppm in air was exposed to contaminate concentrations of at least 200 ppm. No signal response change occurred with carbon monoxide, hydrogen, Freon 114 B-2, ammonia, methane, and acetaldehyde. There was, however, a signal reduction on exposure to $NO_2$ and increases when exposed to acetone and several amines (butyl-, propyl-, diethyl-, dipropyl-). The response change in the presence of $NO_2$ reflects the mutual reactivity of these two materials. The signal diminution of MMH at 100 ppm with $NO_2$ concentration is shown in Figure 23. The signal diminution is shown in terms of signal height (as recorded on the Honeywell Electronik 19 recorder) and as a percentage of the signal resulting from MMH alone. At 500 ppm of $NO_2$ the signal is reduced to about one-fourth. Diminution begins at about 4 ppm of $NO_2$.

The response changes associated with acetone and amines are peculiar to the previously discussed logic scheme used for detecting MMH and $NO_2$. Both acetone and the amines yield fragments of mass 45. Even though the electron energy in the ionizer is low (14.8 ev) to reduce fragmentation, some fragmentation of these compounds occurs because they have relatively low ionization potentials themselves.

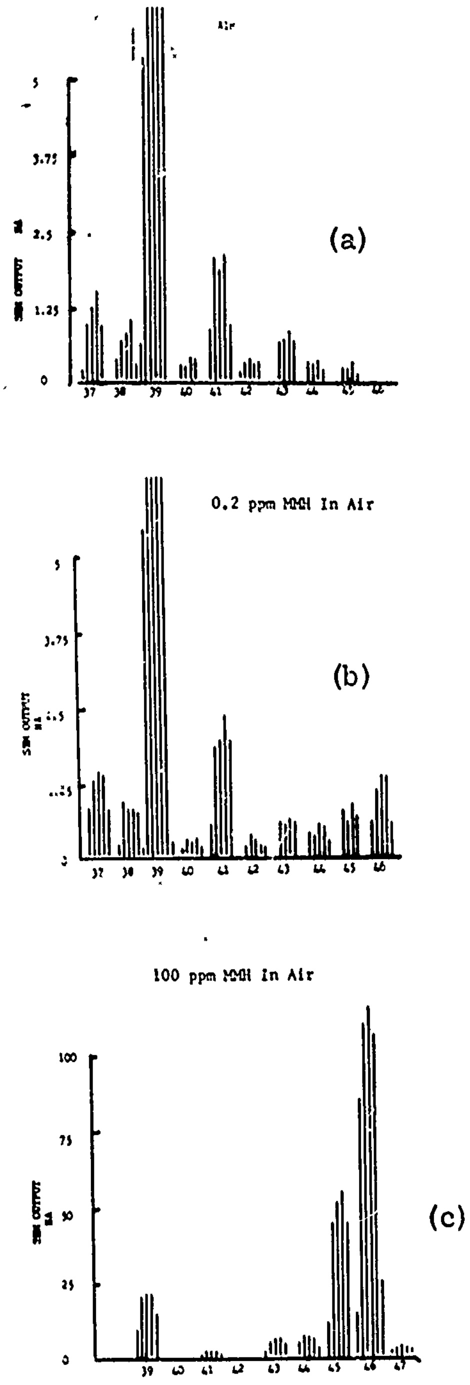

Figure 20. Replica of Pulsed Mode Mass Spectra of Air, MMH, and $NO_2$

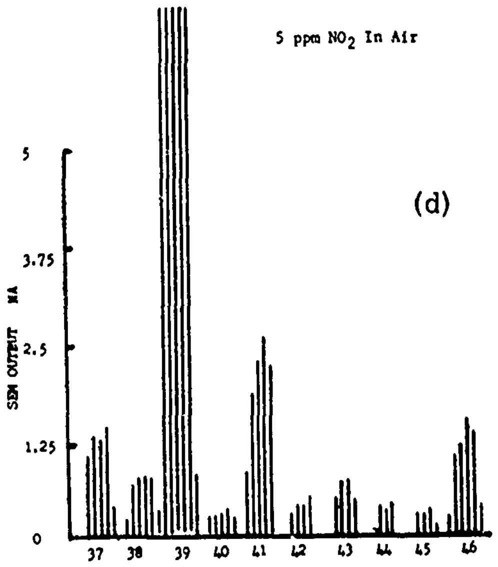

500 ppm $NO_2$ In Air

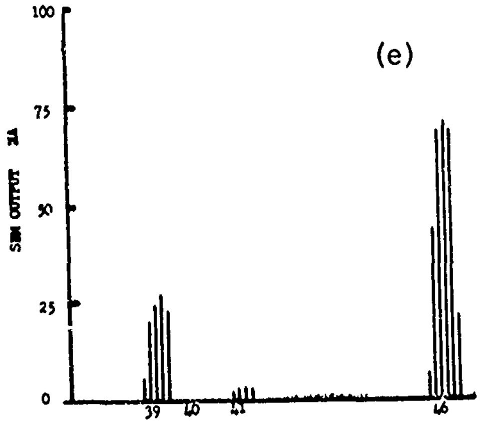

Figure 20. Replica of Pulsed Mode Spectra of Air, MMH, and $NO_2$ (Concluded)

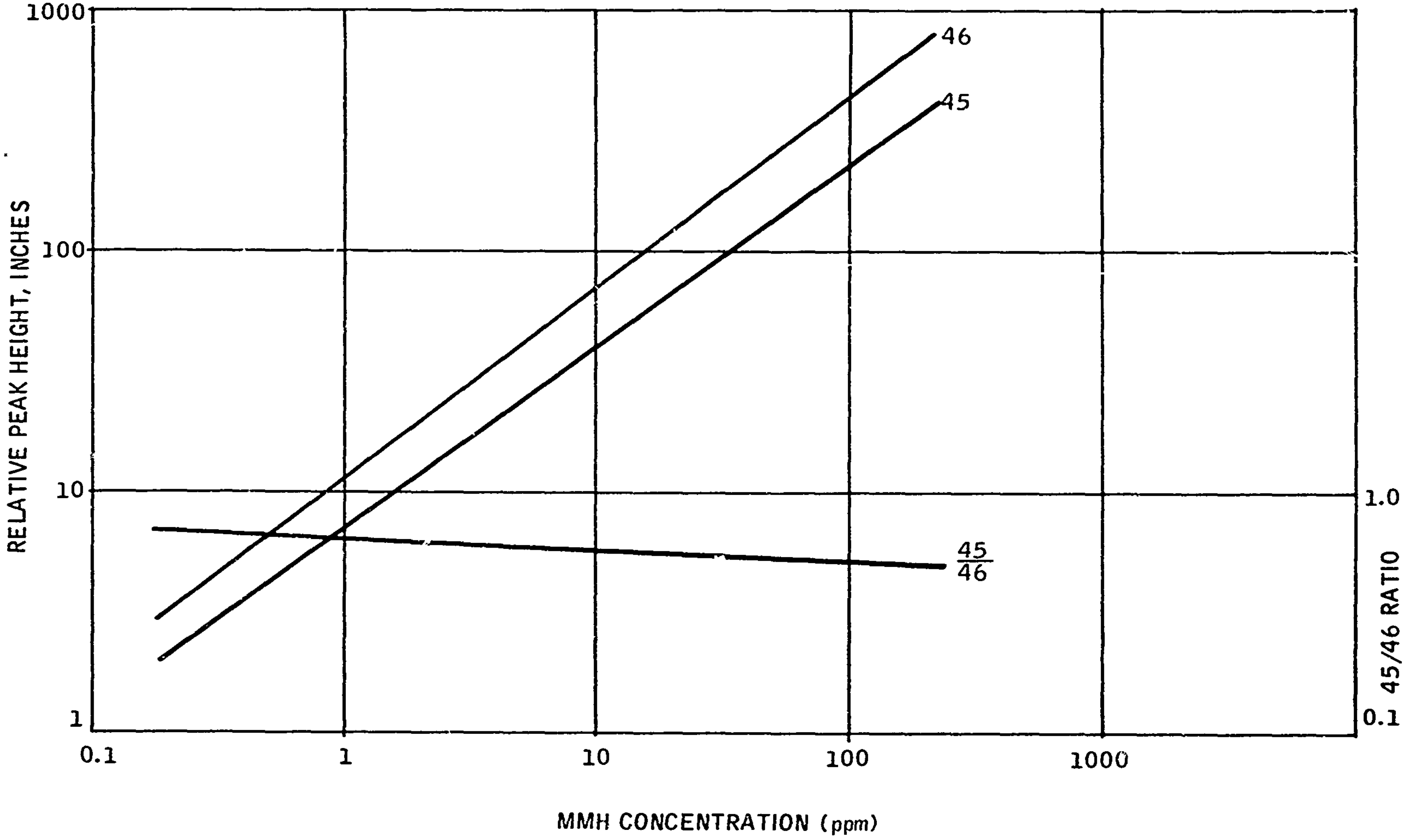

Figure 21. Mass 45 and 46 Peak Heights of MMH at Low Concentrations in Air

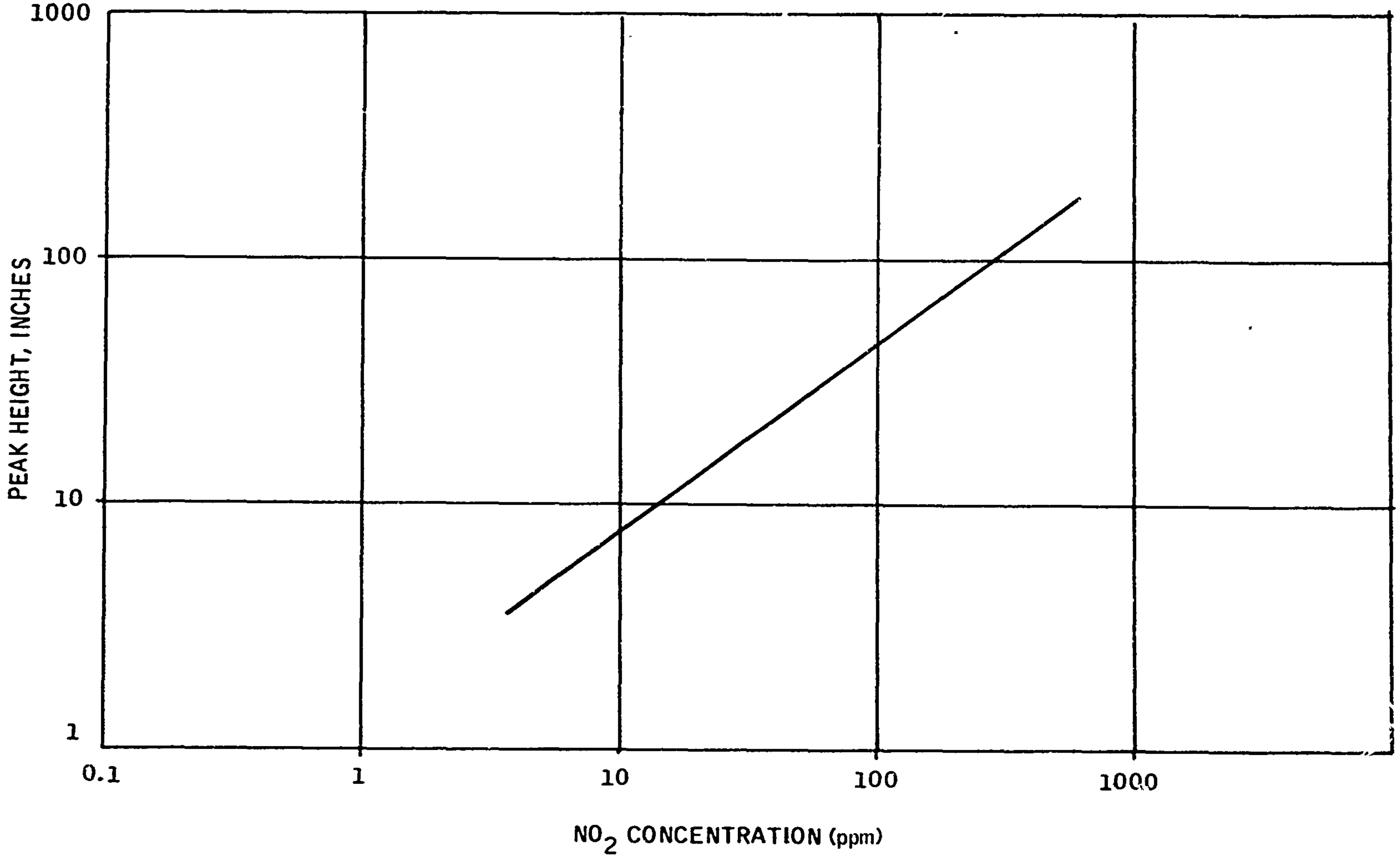

Figure 22. Mass 46 Peak Height versus Concentration (In Air)(14 ev Electron Energy)

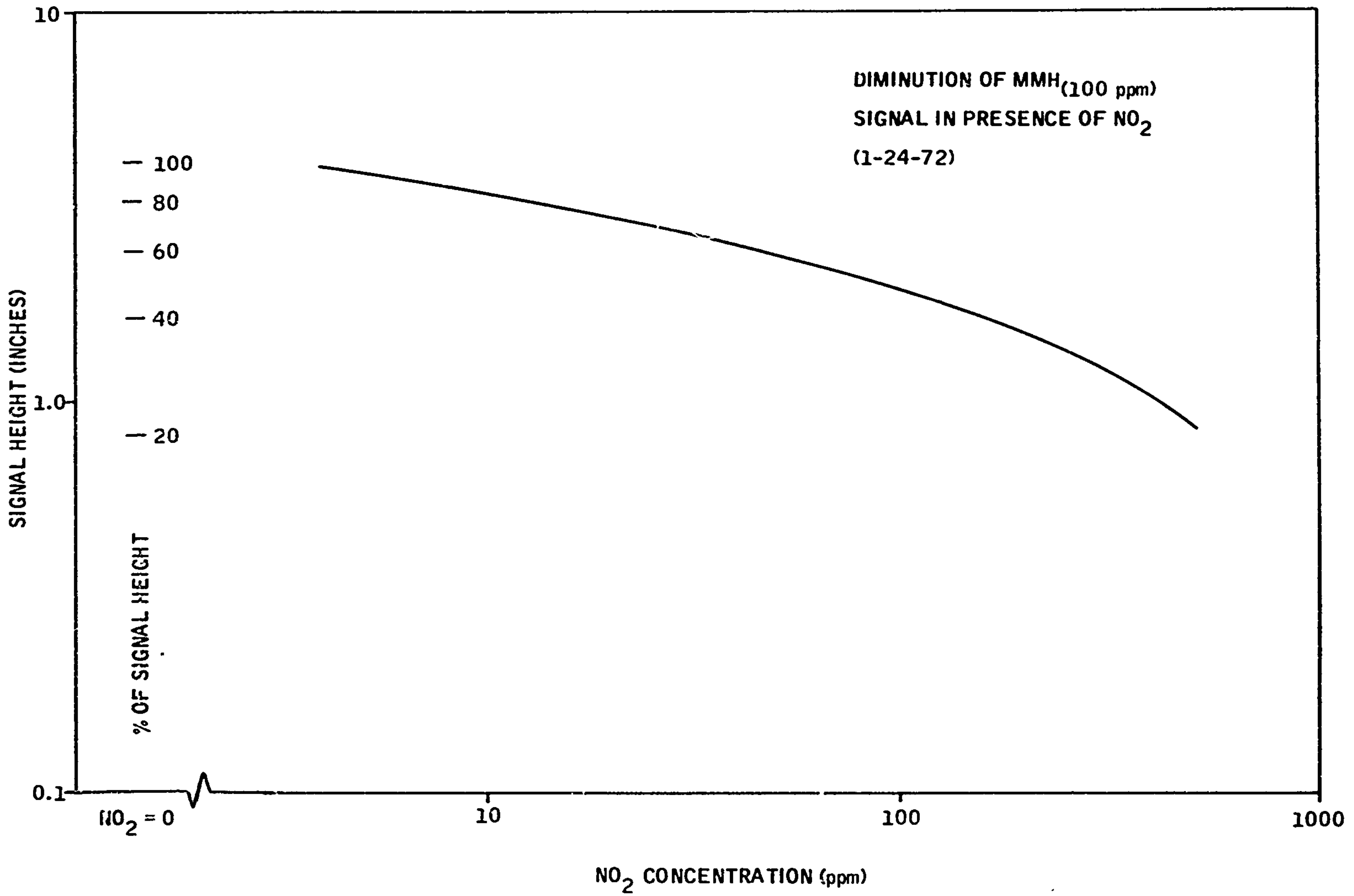

Figure 23. Diminution of MMH (100 ppm) Signal in Presence of $NO_2$

Table VIII. MMH/Contaminate Testing Summary

| Contaminate (≥ 200 ppm) | Effect on MMH Signal (100 ppm) |
|---|---|
| NO | Reduces to ~ 1/3 |
| CO | None |
| $H_2$ | None |
| Freon 114 B-2 | None |
| $NH_3$ | None |
| $CH_4$ | None |
| Aldehyde (acetaldehyde) | None |
| Ketone (acetone) | Increases ~ 10% |
| Amine (butyl-) | Increases 15 to 50% |
| Amine (propyl-) | Increases 15 to 50% |
| Amine (diethyl-) | Increases 15 to 50% |
| Amine (dipropyl-) | Increases 15 to 50% |

Table IX is the testing summary for $NO_2$ response in the presence of contaminates. $NO_2$ at 500 ppm in air was exposed to the several contaminantes at concentration levels of at least 200 ppm (except for MMH at 100 ppm --the maximum of the detection range specified). There were no interferences in the presence of carbon monoxide, hydrogen, Freon 114 B-2, ammonia, methane, acetone, butylamine, and dipropylamine). There were interferences with MMH, acetaldehyde, propylamine, and diethylamine. The diminution of $NO_2$ signal response in the presence of acetaldehyde, whose molecular weight is 44, reflects a reaction in which fragments of amu 45 result. All four of the amines tested, as well as ammonia, produced visible aerosols in the mixing chamber through which the sample gas flowed. However, the reactions with $NO_2$ were so small that they were not detected by the PGA except for propylamine and diethylamine. The reaction of $NO_2$ with the other amines and ammonia did not diminish the $NO_2$ significantly. Data on interference testing was taken with the subsequently developed MMH-$NO_2$ display/control panel which monitors mass numbers 45 and 46 and, through logic, produces an analog signal for each compound (MMH and $NO_2$). This instrumentation is described elsewhere in this report.

Table IX. $NO_2$/Contaminate testing summary

| Contaminate (≥ 200 ppm) | Effect on $NO_2$ Signal (500 ppm) |
|---|---|
| MMH (100 ppm) | Reduces ~ 30% |
| CO | None |
| $H_2$ | None |
| Freon 114 B-2 | None |
| $NH_3$ | None * |
| $CH_4$ | None |
| Aldehyde (acetaldehyde) | Reduces to zero |
| Ketone (acetone) | None |
| Amine (butyl-) | None |
| Amine (propyl-) | Slow, Steady Decrease * |
| Amine (diethyl-) | Slow, Steady Decrease * |
| Amine (dipropyl-) | None * |

*Slight Aerosol Formation Visible in Mixing Chamber

Table X is the humidity-testing summary. Extreme humidities have no effect on signal response except for MMH at 95 percent relative humidity. At this condition the MMH signal was one-half that at room relative humidity (about 10 percent RH). Vernot, et al.[4], have suggested the possibilities of hydrate formation when MMH is exposed to humid air, but little is known about MMH-water vapor reactions. A sketch of the sample dilution apparatus as used for high humidity testing has been shown in Figure 16. With this apparatus there is a possibility for several seconds of exposure of MMH to the humid air in the mixing chamber. As noted previously, $NO_2$ was exposed to high and low humidities by flushing 5-liter bottles with dry or humid air prior to injection the $NO_2$. With this method no variation of $NO_2$ signals was noted.

As part of the test plan for the PGA laboratory model, the instrument was operated while exposed to environmental temperature of 0°F and +125°F. Departures from normal operation were noted during the cold temperature tests with MMH and $NO_2$. Table XI shows the temperature-testing summary.

---

[4] Vernot, E.H. et al.: The Air Oxidation of Monomethylhydrazine, J. Amer. Ind. Hyg. Assoc., Vol. 28, page 343, 1967.

The mass spectrometer was enclosed in an insulated box connected to a temperature control chamber by 4-inch ducts. The temperatures were varied between 0°F and 120°F while the mass spectrometer sampled MMH at 50 ppm and $NO_2$ at 250 ppm. The response to both compounds was virtually eliminated at 0°F.

To determine whether this was due to a change in instrument operation as temperatures were lowered or a condensation effect, pulsed air spectra were taken while repeating the temperature variations. In the temperature range of 18°F to 95°F (temperature of metal case), the peaks at amu 28 ($N_2$), 32 ($O_2$) and 40 (A) did not vary. Amu 42 (unidentified) did not vary over the temperature range 5° to 110°F.

Table X. Humidity Testing Summary

| Condition | Relative Humidity | | |
|---|---|---|---|
| | 5% | Room | 95% |
| MMH (1 ppm) | No Response Change | | Response Halved |
| MMH (50 ppm) | No Response Change | | Response Halved |
| $NO_2$ (7.5 ppm) | ←—— No Response Change —— | | |
| $NO_2$ (250 ppm) | ←—— No Response Change —— | | |

Table XI. Temperature testing summary

| Condition | Temperature, °F | | | | |
|---|---|---|---|---|---|
| | 0 | 40 | 70 | 90 | 125 |
| 1-High Scale | | | | | |
| MMH (50 ppm) | No Response | ←— No Response Change —→ | | | |
| $NO_2$ (250 ppm) | No Response | ←— No Response Change —→ | | | |
| 2-Air Spectrum Peaks ($N_2$, $O_2$, A) | ←— No Response Change —→ | | | | |
| 3-Low Scale MMH (1 ppm) | ←— No Data Obtained —→ | | | | |
| $NO_2$ (7.5 ppm) | ←— No Data Obtained —→ | | | | |

Investigation was also made of extreme temperature performance of secondary emission multipliers to determine if the loss of signal response at O°F might be from this cause. According to DuMont Laboratories, there is no change in the ratio of the number of electrons leaving a dynode surface to the number incident over a temperature range from 0° to 1700°C for those metals they have tested. From this information it is believed that the loss of MMH and $NO_2$ signal at 0°F does not result from SEM temperature differences. This would suggest that reduction in response to MMH MMH and $NO_2$ was due to condensation effects.

A possible explanation for this signal reduction at low temperature is that the sample materials were condensing in the cold inlet passages of the PGA since the mass peaks of nitrogen, oxygen, and argon continued to occur. It is noted that MMH has a boiling point of 87°C while $NO_2$ changes to $N_2O_4$ at about 20°C. The low scale range temperature tests were not run at this time because of the lack of sensitivity problem. Figure 18 shows a copy of the actual recorder trace of the MMH response while varying the temperature. Figure 19 shows copies of Visicorder records made while sampling $NO_2$ at low temperature. The difference in height of the $CO_2$ peaks (amu 44) is due to the use of dry ice in the room while producing a cold environment.

Subsequent to the environmental and temperature testing, a deterioration of the sensitivity performance of the PGA laboratory model was noted. This deterioration is thought to be due to contamination of the surfaces of the SEM detector after several months of hard use. The model was then baked out - a common practice in mass spectroscopy when continued exposure to air is encountered. After bake-out, it was determined that the secondary emission multiplier was less sensitive and noisy. The defective unit is being replaced.

Pulsed mode mass spectra of several compounds other than MMH and $NO_2$ have been taken during the course of the program. Some of these were from the list of possible interfering compounds supplied by RPL. This list is given in Table XII.

Table XII. Possible interfering compounds

| Compound | Molecular Weight |
|---|---|
| Freon 114 B-2 | 260 |
| Ketone (Acetone) | 58 |
| Aldehyde (Acetaldehyde) | 44 |
| Amines (primary and secondary) | --- |
| Carbon monoxide | 28 |
| Hydrogen | 2 |
| Ammonia | 17 |
| Methane | 16 |

Spectra were taken of Freon 114 B-2 and acetone. Other than interference testing, no spectra were taken of the amines. Since acetaldehyde, carbon monoxide, hydrogen, ammonia, and methane all have molecular weights lower than MMH and $NO_2$ and predictably simple spectra, they were not mass analyzed. In addition, some spectral analysis was done on methanol ($CH_3OH$), and ethanol ($C_2H_5OH$). Some Visicorder records of these spectra are shown in Figures 24 to 26. Since they were done at different times, the mass range and peak heights are different on individual records. The most comprehensive spectra were of Freon 114 B-2. All of these spectra show the peaks normally found in air in addition to the peaks due to the compound.

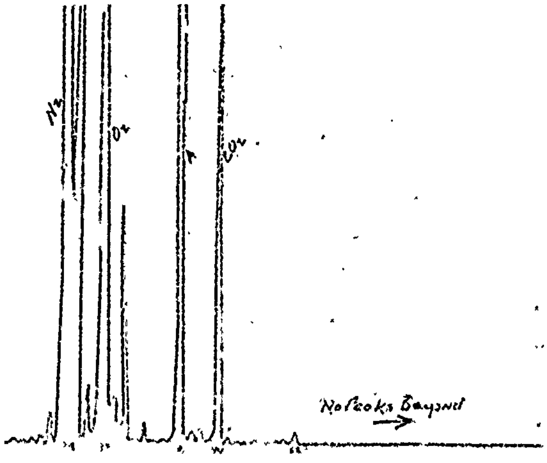

Air

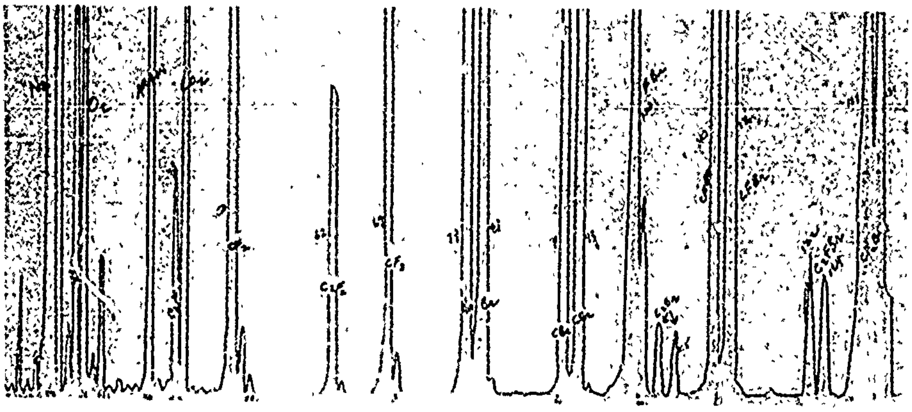

Freon 114B-2 in Air

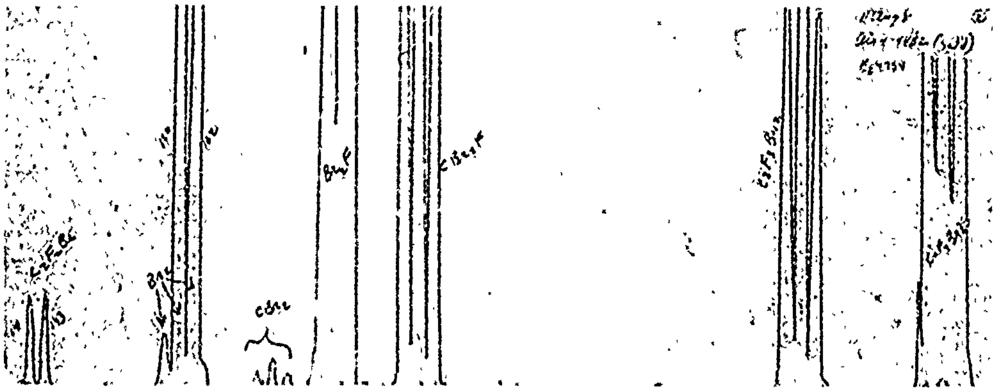

Freon 114B-2 in Air

Figure 24. Replica of Freon 114B-2 Spectra

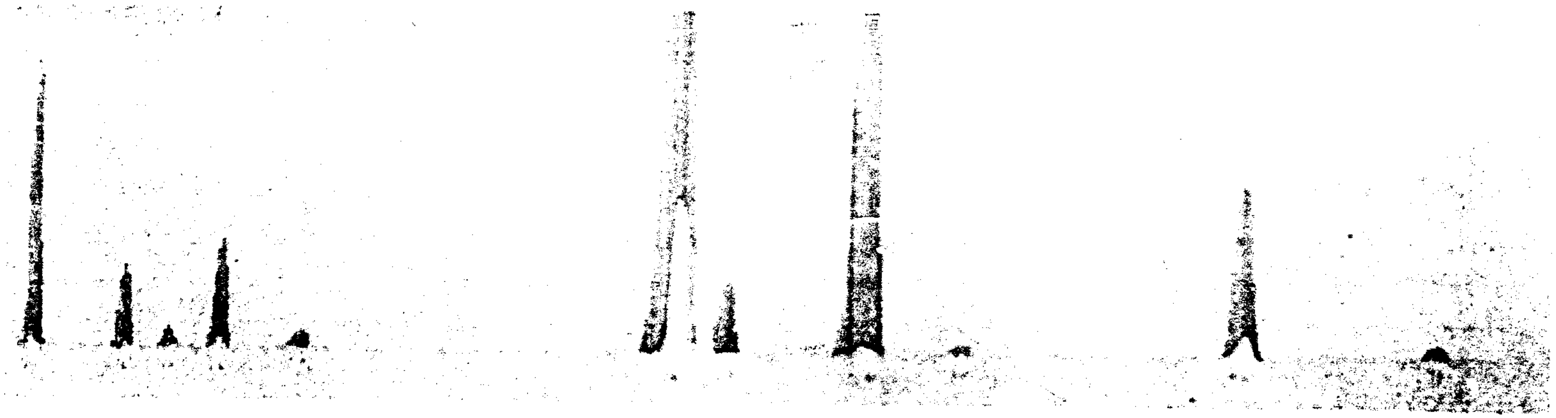

Air

Ethanol in Air

Figure 25. Replica of Ethanol Spectra

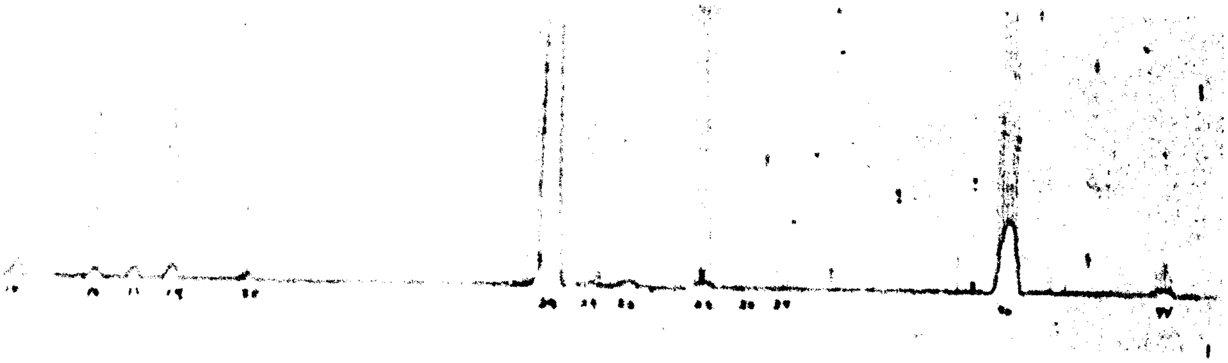

Air

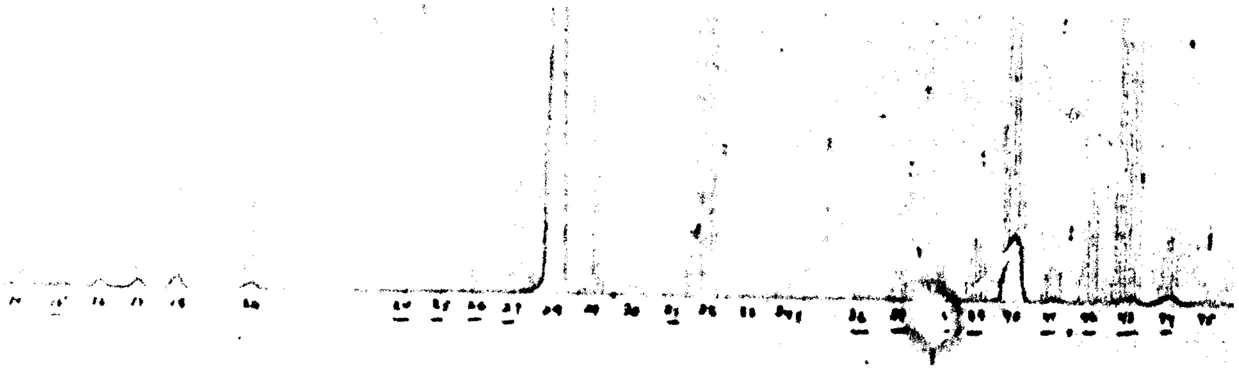

Acetone in Air

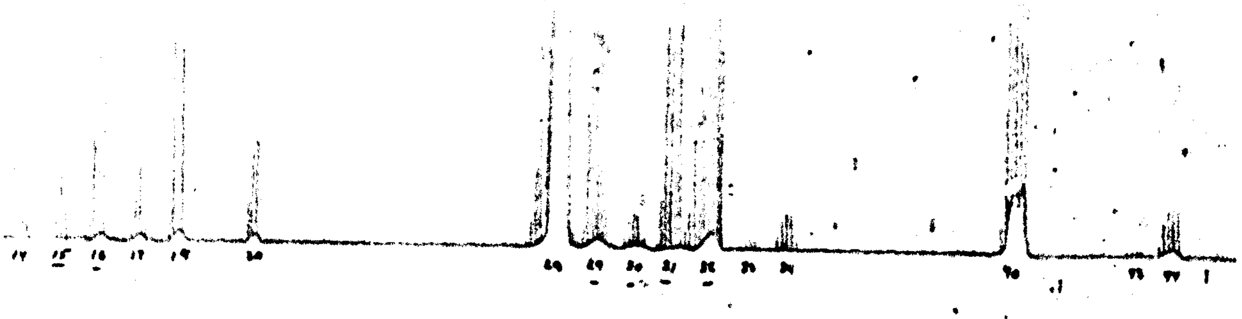

Methanol in Air

Figure 26. Replica of Acetone and Methanol Spectra

# SECTION XIII

# INTERNAL COMBUSTION ENGINE EMISSIONS EXHAUST GAS TESTING WITH THE PGA LABORATORY MODEL

Since internal combustion engines may be in the proximity of Minuteman III operations, there is the requirement that detection of any MMH and $NO_2$ leakage not be compromised by the presence of internal combustion engine emissions. Such emissions consist of water vapor and carbon dioxide, which are normally present in the atmosphere, as well as carbon monoxide, hydrocarbons, and nitrogen oxides. Other gases in lesser amounts, such as aldehydes and ketones, may also be emitted or formed subsequently in atmospheric reactions. Of these gases only those of concern in the use of the PGA as a toxic vapor detector would be the ones having a molecular weight, or a fragmented ion mass, whose mass numbers coincide with those used in monitoring MMH or $NO_2$.

Exhaust gases from three cars and three diesel trucks were taken as bag samples directly from the tail pipes. These gases were then admitted to the inlet of the PGA laboratory model. Since no dilution was made of the samples, this test was more severe than would be the case in actually monitoring MMH/$NO_2$ leakage. Mass spectra were taken in the range of 36 to 46 atomic mass units (amu); i.e., the region including the mass numbers used for monitoring and self-calibrating the PGA toxic vapor detector. The results of this test are summarized in the following paragraphs.

## SPARK-IGNITION ENGINES

The occurrence and magnitude of mass peaks in the spectra (amu 36 to 46) of undiluted exhaust gas taken at "idle" were similar for three quite different cars (1966 Mustang, 1964 Buick V6, and 1969 Sunbeam).

One car was equipped with automatic transmission and could be lightly loaded. The load peaks were generally less than the idle peaks.

No amu 46 peak was observed except for the one car under load. This observation suggests that little $NO_2$ was present, and is supported by the work of others who have reported that most $NO_x$ emission is NO (Refs. 1, 2, 3). The magnitude of this amu 46 peak was about equal to that produced by 0.2 ppm MMH or 5.3 ppm $NO_2$.

There were small amu 45 peaks present in all cases - about equal to those occurring with 4.5 ppm MMH.

No false indication of the presence of MMH would occur, because of the high amu 45-to-amu 46 ratio.[5] The measurement of MMH and $NO_2$ leakage might possibly be impaired were the measurement made very near the tailpipe of an internal combustion engine. However, dilution of the exhaust by a factor of 25 or more would eliminate this possibility since the amu 45 peak would then be lower for exhaust gas than for MMH in the least concentration which must be detected.

The testing of these three cars agrees with earlier qualitative testing using low (14 ev) electron energy with another ion source configuration. The group of peaks occurring in the 39 to 45 amu range is apparently due to $C_3$ hydrocarbons and is separate and distinct in the low electron energy mass spectrum from the $C_2$ and $C_4$ groups which also appear. The limited testing suggests that these groups in the spectrum narrow and the peaks become less as an engine is loaded.

The carbon dioxide isotopic peak at amu 45 is adequately suppressed by use of low electron energy ionization so that no interference in MMH detection occurs using this mass number.

## DIESEL ENGINES

The pattern of peak occurrence in the mass spectra of raw exhaust gas taken at "idle" was the same for three diesel engines (International CO 4000, International Fleetstar 2000, and Mack) used as tractors for semi-trailers in the 70,000 GW class.

In the range of interest, peaks occurred at amu 41, 42, 43, 44, 45, and 46, with 42, 44, and 46 being more predominant. These peaks were greatly reduced in the mass spectra of day-old exhaust gas samples.

The amu 46 peaks occurring in the three diesel exhaust spectra were equivalent in height to those occurring with $NO_2$ at concentrations of 15 to more than 56 ppm. The latter would require dilutions greater than 11 times to eliminate every possibility for interference with $NO_2$ leakage measurement. The amu 45-to-amu 46 ratios were less than 0.5 for two of the three diesel engines.

---

[5] MMH would only be indicated if this ratio is 0.5 or less.

## DILUTION OF INTERNAL COMBUSTION ENGINE EXHAUST IN THE ATMOSPHERE

In the outdoor atmosphere the tailpipe plume will quickly attain the velocity of the prevailing wind, and its rise will be determined by any vertical momentum and buoyancy due to heat and molecular weight difference. Dispersion will come about first by the turbulence created by the relative motion of the plume and atmosphere and then by the turbulence of the atmosphere itself. Estimates of the concentration of exhaust gas components in the atmosphere based on conventional plume dispersion theory are shown in Figure 27. This figure shows that dilution is affected by engine load condition (source strength) and weather conditions.

Dilutions of 10 to 300 may occur within 10 meters downwind of the exhaust location. Such dilution apparently would be adequate to remove the possibility of interference with MMH and $NO_2$ measurement using amu 45 and amu 46. Should this not be the case, it would be necessary to use additional mass number(s) and logic for the toxic vapor detector. In this connection the mass peaks associated with spark-ignition and diesel engine exhaust gases were examined to determine which mass peaks were associated with both of these types of exhaust gas but not MMH or $NO_2$. By adding such a mass number to the detection circuitry programming, it would be possible to present an alarm readout were exhaust gas present. In the 39 to 43 mass region, amu 42 was the dominant peak for the spark-ignition engines, followed by amu 43. Amu 43 was the highest peak for the diesel engines, followed by amu 42. Based on this limited testing, amu 42 would be the better peak to use as an exhaust gas indicator since there is apparently negligible response to MMH, $NO_2$, and the specified contaminates at this mass number.

## CONCENTRATIONS OF VEHICLE-ASSOCIATED GASES IN THE ATMOSPHERE

Upon release, internal combustion engine exhaust gases are subjected to physical and chemical processes in the atmosphere, and their concentrations in a polluted atmosphere are indicated by the data of the Continuous Air Monitoring Program (CAMP). Table XIII shows the frequency distribution of concentrations of carbon monoxide, nitric oxide, nitrogen dioxide, total hydrocarbons, and total oxidant in the six cities monitored by CAMP. The concentration values shown are the arithmetic mean of 5-minute averages over a 1-year period.

Table XIII shows that nitrogen dioxide concentration may be as high as 0.09 ppm and nitric oxide concentrations as high as 0.2 ppm. The California air quality network in a recent report (Ref. 4) cites a maximum hourly average in the South Coast Basin for nitric oxide in the order of 1 ppm and fo nitrogen dioxide up to 0.5 ppm. Apparently oxides of nitrogen emissions are

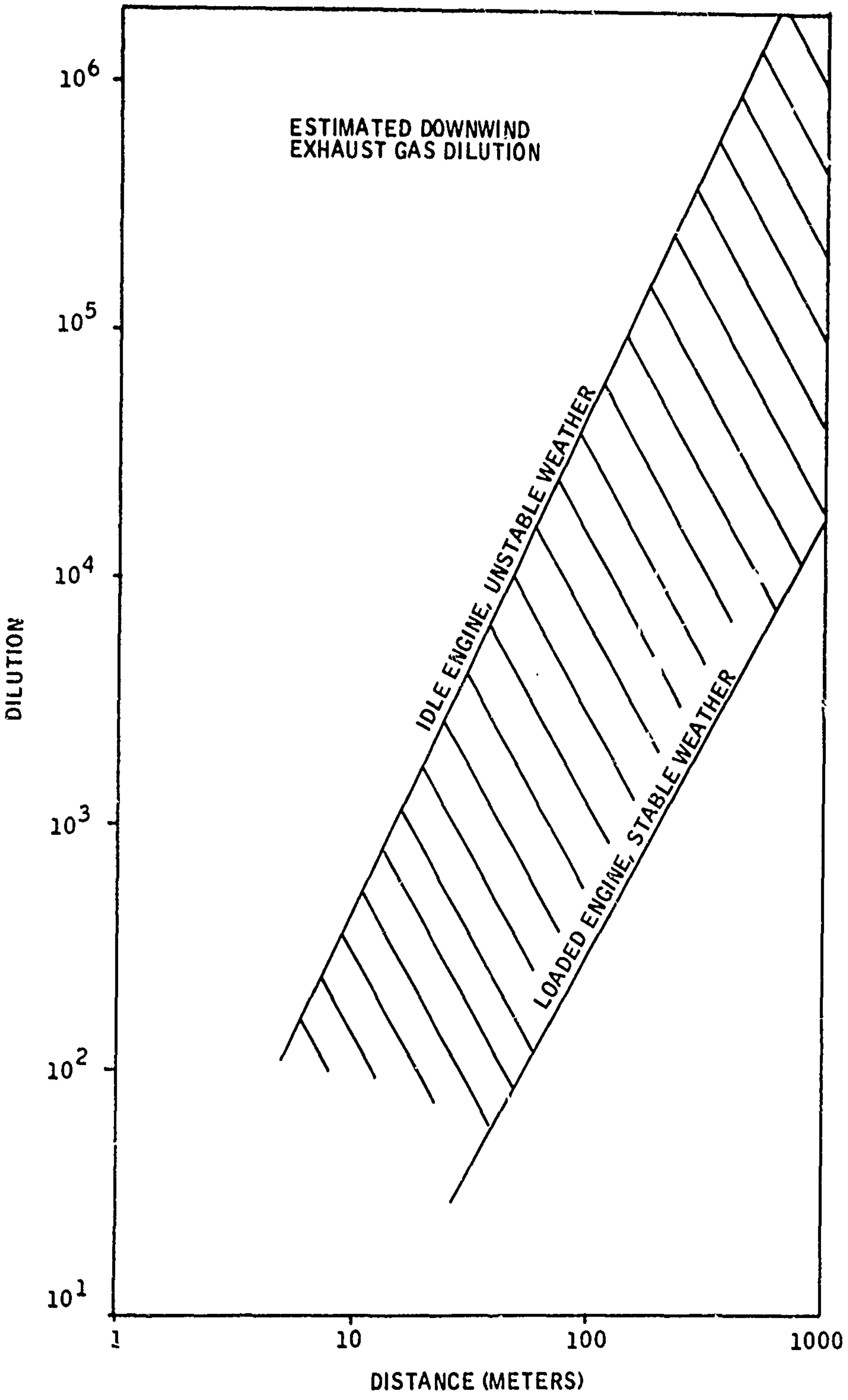

Figure 27. Estimated Downwind Exhaust Gas Dilution

Table XIII. Frequency Distribution of Vehicle-Associated Gases in Polluted Atmospheres*

| | Carbon Monoxide | | Nitric Oxide | | Nitrogen Dioxide | | Total Hydrocarbons | | Total Oxidant | |
|---|---|---|---|---|---|---|---|---|---|---|
| Concentration | 10% | 90% | 10% | 90% | 10% | 90% | 10% | 90% | 10% | 90% |
| Maximum Concentration City | 5 | 22 | 0.02 | 0.2 | 0.03 | 0.09 | 2 | 4.4 | <0.01 | 0.07 |
| Minimum Concentration City | 1 | 6 | <0.01 | 0.08 | 0.01 | 0.05 | 1 | 2.9 | <0.01 | 0.04 |

* % of time concentration is equal to or less than indicated concentration. Yearly arithmetic mean, 5-minute averaging time, in six cities monitored by the Continuous Air Monitoring Program, 1966.

short lived in the atmosphere and background levels are low. One estimate (Ref. 5) places the concentration of NO in the troposphere away from major sources in the order of 0.01 ppm, and another (Ref. 6) suggests comparable concentrations of NO and $NO_2$ in remote areas.

Table XIII also shows that carbon monoxide concentration may be up to 22 ppm in polluted atmospheres. The California air quality network report (Ref. 4) cites a maximum hourly average for the South Coast Basin for CO as high as 41 ppm. Junge (Ref. 7) has estimated the atmospheric background level of CO to be in the range of 0.01 to 0.20 ppm.

Total hydrocarbons concentration may be as high as 4.4 ppm according to the CAMP data. The volatility of hydrocarbons is approximately determined by their carbon number (number of carbon atoms in each molecule). Hydrocarbons having a carbon number of 1 to 4 are gaseous at ordinary temperatures. Higher carbon number hydrocarbons are liquids or solids in the pure state, and those having a carbon number greater than 12 are generally not sufficiently abundant to reach troublesome atmospheric concentrations in the gas phase. One summary (Ref. 8) lists individual hydrocarbons detected in urban air by gas chromatographic analysis as follows:

| Carbon Number | Number of Compounds Found |
|---|---|
| 1 | 1 |
| 2 | 3 |
| 3 | 4 |
| 4 | 7 |
| 5 | 11 |
| 6 | 16 |
| 7 | 5 |
| 8 | 4 |
| 9 | 4 |
| 10 | 1 |

This listing shows the most prevalent hydrocarbons are those having five or six carbon atoms per molecule.

In Los Angeles smog, hydrocarbon concentrations may be in the region of 0. 1 to 0. 5 ppm. These are subject to diurnal variation with a morning peak and lowest concentrations in the absence of sunlight. Some of the irritating effects of smog are caused by the presence of formaldehyde and acrolein which may be present in Los Angeles in concentrations up to 0. 12 ppm and 0. 009 ppm, respectively. Junge (Ref. 7) cites a concentration range from 0 to 0. 01 ppm for formaldehyde in the normal atmosphere.

Leighton (Ref. 9) points out the diurnal variation in pollutant concentrations which reflects the pattern of human activity and solar radiation. On days producing eye irritation in Los Angeles, an initial peaking of NO of 0. 1 to 0. 2 ppm in the early morning hours is followed in order by peaks of $NO_2$ (~0. 2 ppm), hydrocarbons (~0. 5 ppm), aldehydes (~0. 3 ppm), and ozone (~0. 2 ppm) by early afternoon.

Data on aldehyde concentrations are poorly quantified and by far most of the available data are from Los Angeles. The range of yearly maximum 1-hour average concentrations of total aldehydes was from 0. 20 to 1. 30 ppm in the years from 1951 through 1957 and of formaldehyde from 0. 05 to 0. 12 in 1951 (Ref. 10). The maximum acrolein value was 0. 011 ppm during a period from July to November, 1960, with most values being less than half this amount.

Aldehydes are major end products of atmospheric photochemical reactions involving reactive hydrocarbons and nitrogen oxides. But they are also present directly in vehicle exhaust gas, though relatively little analytical work has been reported. Ketones are thought to be very minor components relative to aldehydes. Oberdorfer (Ref. 11) has reported aldehyde emission data for a limited number of vehicles with and without exhaust control systems. Using the 7-mode California cycle as a basis for his testing, Oberdorfer reports total aldehydes from 18 ppm to 275 ppm, depending on engine operation mode, emission control device configuration, and engine parameter settings. One analysis of individual aldehydes and ketones is given in Table XIV.

Table XIV. Analysis of Individual Aldehydes and Ketones (Ref. 11) V8 Engine Exhaust

| | Mole % |
|---|---|
| Formaldehyde | 70.2 |
| Acetaldehyde | 7.2 |
| Propionaldehyde and acetone | 0.4 |
| n - Butyraldehyde | 0.4 |
| iso - Butyraldehyde | trace |
| n - Valeraldehyde | 0.4 |
| iso - Valeraldehyde | trace |
| 2 - Ethylbutyraldehyde | trace |
| Acrolein | 9.8 |
| Crotonaldehyde | 0.4 |
| Methacrolein | trace |
| Benzaldehyde | 8.5 |
| Other $C_7$ + aldehydes as $C_7$ | 2.5 |

As seen in Table XIV, formaldehyde is the principal component while ketone concentrations are negligible.

## SECTION IX

## INTERPRETATION OF FINDINGS AND RECOMMENDATIONS

The PGA laboratory model has been operated approximately 1000 hours with about 2 million gas sample admissions during the course of the feasibility study. Mass spectral data have been taken on more than a dozen gases and gas mixtures. Techniques have evolved for operating the vacuum and electronics systems and for observing performance under a variety of test conditions. An equipment evaluation/performance summary is given in Table XV.

Table XV. Equipment Evaluation/Operation Summary

| | |
|---|---|
| Data Recording: | 94 days |
| Spectra Recording: | 17 gases |
| MMH and $NO_2$: | |
| ● Delivery Technique | |
| ● Spectra Evaluation | |
| ● Signal Response versus Concentration | |
| Pulsed Leak Configurations | (2) |
| Pulsed Leak Calibration | |
| Ion Source Configurations | (4) |
| Signal Amplification Configurations | (4) |
| Power Supply Configurations: | |
| ● Ion Source | |
| ● Secondary Emission Multiplier | |
| Test Variables: | |
| ● Sample Concentrations | |
| ● Pulsed Leak: Dwell, Frequency | |
| ● Electron Emission and Energy | |
| ● Ion Energy and Focus | |
| ● System Pressure | |
| ● Mass Filter Resolution | |
| ● SEM Excitation | |

Table XV shows that two pulse leak configurations were used. These are very similar, however, differing only in that an improvement was incorporated so that only stainless steel surfaces were exposed to the sample gas. The only maintenance required for the pulsed leaks was on two or three occasions after system start-up and degassing when excessive heat application apparently caused heat flow of the poppet material and loss of seating preload. This resulted in seat leakage which was eliminated by re-establishing the preload. No further difficulties have been experienced. The pulsed leak configuration proposed for the PGA breadboard model is essentially the same, but with shorter and more direct sample gas passages.

Table XV also shows that four ion source configurations were used, although two of these were minor modifications made to the second ion source configuration. The ion source is a key component in the PGA, and sensitivity performance may be improved by design optimization should minimum detection thresholds become lower in the Minuteman III, or other, applications. It is noted that the two basic ion source configurations were commercial designs for mass spectrometers and used "as is". It is useful to note that no filament "burn outs" occurred during the test program and that filaments can withstand pulsed-mode gas sample introduction from atmospheric pressure. For the PGA breadboard model it is recommended that the ion source be essentially similar to the No. 1 configuration. This is a simple design needing a minimum of power supplies. Improved sensitivity performance will be sought by enclosing the ionizing region.

Near the end of the test program a loss of detection sensitivity was noted. This has been attributed to contamination of the SEM detector dynode surfaces after the several months of comparatively hard use in air sampling (some 2 million cycles). A replacement detector is to be installed and sensitivity performance will be verified. It may be that SEM life is limited to about 1000 hours in this service, although no conclusions can yet be drawn. In the interest of achieving miniaturization, it is recommended that a Channeltron electron multiplier be used in the development of the PGA breadboard model.

During the feasibility study a test plan was evolved and used as a basis for determining the effects of extreme temperatures and humidities on PGA performance as well as the effects of the specified contaminates in the atmospheric sample. The results have been discussed in Section VII. A testing summary is shown in Table XVI. The underlined tests have been completed. It is seen that 48 of the 61 tests proposed have been completed. The testing was curtailed because of the degraded sensitivity performance of the PGA laboratory model. The low-scale MMH performance under temperature extremes may possibly be anticipated in view of the high-scale results (i. e., cold will diminish the response, hot will have no effect). Storage temperature tests may be superfluous since extreme temperature exposures would be expected to produce no changes in the materials of construction and configuration of the PGA after restoration of normal temperature. After

Table XVI. Testing Summary

| | Low Scale | | | | | | High Scale | | | | | | |
|---|---|---|---|---|---|---|---|---|---|---|---|---|---|
| | MMH(ppm) | | | $NO_2$(ppm) | | | MMH(ppm) | | | $NO_2$(ppm) | | | |
| | 0.2 | 1.0 | 2.0 | 5.0 | 7.5 | 10 | 10 | 50 | 100 | 20 | 250 | 500 | No. Runs |
| Room Ambient | | | | | | | | | | | | | |
| @ Room R. H. | X | X | X | X | X | X | X | X | X | X | X | X | 12 |
| @ 5% R. H. | | X | | | X | | | X | | | X | | 4 |
| @ 95% R. H. | | X | | | X | | | X | | | X | | 4 |
| Temperature | | | | | | | | | | | | | |
| @ + 90°F | | X | | | X | | | X | | | X | | 4 |
| @ + 40°F | | X | | | X | | | X | | | X | | 4 |
| @ + 125°F | | X | | | X | | | X | | | X | | 4 |
| @ 0°F | | X | | | X | | | X | | | X | | 4 |
| Storage Temperature | | | | | | | | | | | | | |
| + 150°F Soak | | X | | | X | | | X | | | X | | 4 |
| - 40°F Soak | | X | | | X | | | X | | | X | | 4 |
| Contaminates | | | | | | | | | | | | | |
| $NO_2$ | | | | | | | | | X | | | | 1 |
| Freon 114B-2 | | | | | | | | | X | | | X | 2 |
| Acetone | | | | | | | | | X | | | X | 2 |
| CO | | | | | | | | | X | | | X | 2 |
| $H_2$ | | | | | | | | | X | | | X | 2 |
| Acetaldehyde | | | | | | | | | X | | | X | 2 |
| $CH_4$ | | | | | | | | | X | | | X | 2 |
| $NH_3$ | | | | | | | | | X | | | X | 2 |
| Amines | | | | | | | | | X | | | X | 2 |
| Total | | | | | | | | | | | | | 61 |

installation of the replacement SEM detector and restoration of normal performance of the PGA, it is suggested that laboratory model testing resume as follows:

- Obtain data on the diminution of MMH response in the presence of $NO_2$ at several concentrations.
- Determine the relative humidity level at which MMH response begins to degrade in humid atmospheres, obtaining mass spectra at the same time to study the little-known reaction chemistry.
- Determine if the low-temperature response degradation with MMH and $NO_2$ is indeed due to condensation of these materials in the sampling passages. If so, the shorter, more direct sample passages proposed for the PGA breadboard model may minimize condensation as would the application of heat to the sample passage (a practical solution already applied in a field instrument for chemical agent detection).

The performance of the MMH-$NO_2$ Control Display Unit in the testing program suggests its continued use in the PGA breadboard model. To date, the feature of argon 38 monitoring for self-calibration has not fully been implemented although the programming has been built-in and its operation checked out in the laboratory model testing. This self-check feature, making use of the fixed argon concentration in the atmosphere, makes it possible to be more tolerant of a design using an electron multiplier detector as opposed to a nonamplifying Faraday cup detector.

Based upon the results of the Phase I efforts, it now seems reasonable to project a PGA breadboard model suitable for testing at AFRPL. Such a model is shown in Figure 28. This configuration is based on preliminary layouts and reflects a design philosophy proceeding on a "minimum-risk" basis; that is, proven components will be used wherever possible. Beyond this design a yet more miniaturized model, making use of specially-designed components, is foreseen for the final portable toxic vapor detector (PVD) configuration. Figure 28 shows that the PGA Breadboard Model size is 13 inches x 13 inches x 9.5 inches, a size compatible with the requirement for portability. It would be transported in two parts, an electronics unit and a vacuum system unit (the former being provided with a hinged cover to protect its control panel). These two units would be electrically connected by short cables. Sample inlet would be by means of a short, direct passage (possibly electrically heated) to the pulsed leak. A small gas sampling pump would provide for sample aspiration.

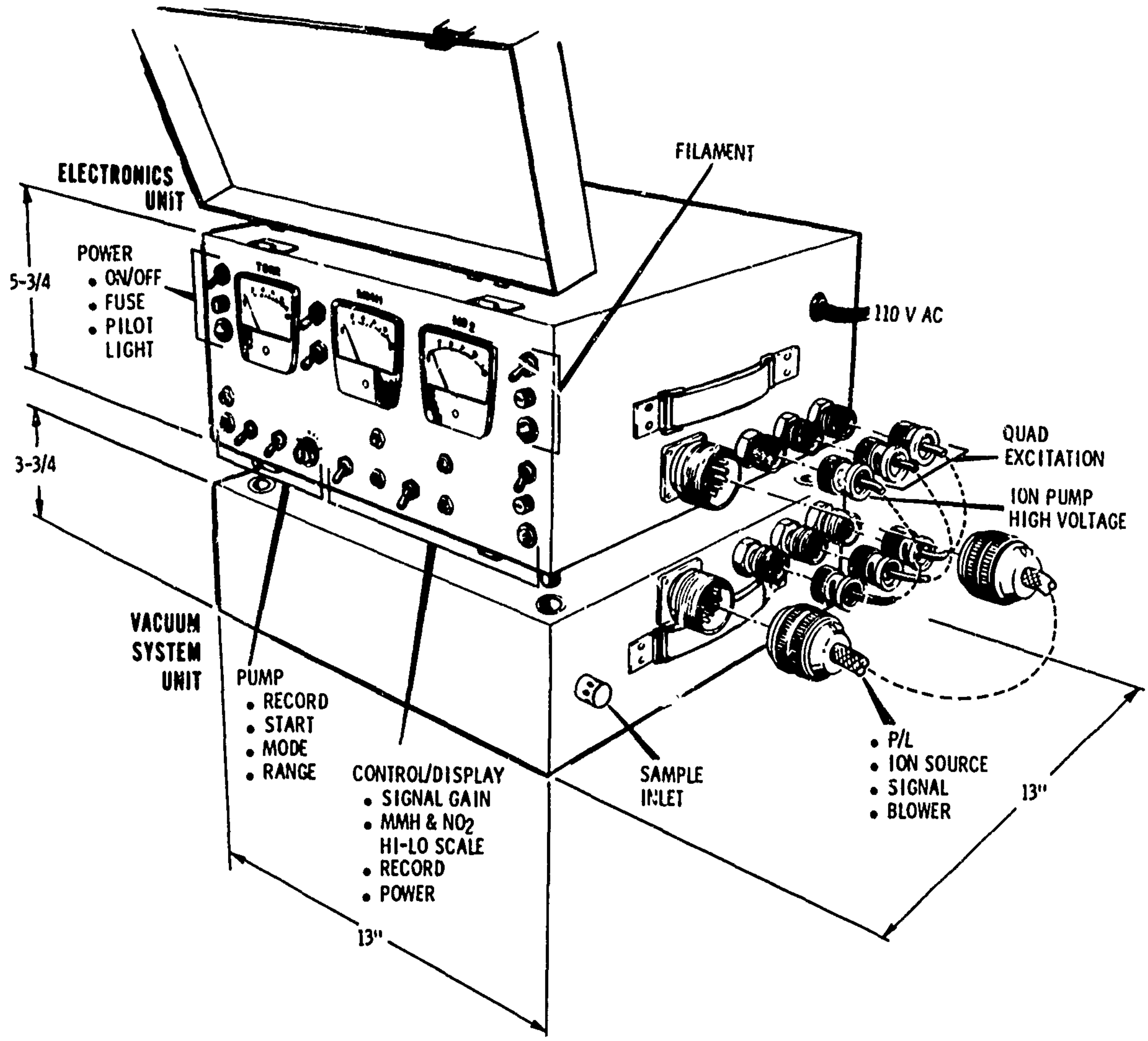

Figure 28. PGA Breadboard Model

# REFERENCES

1. Brown, W.J., et al., "Effect of Engine Intake - Air Moisture on Exhaust Emissions, SAE paper No. 700107, January 1970.
2. Campau, R.M.; and Neerman, J.C., "Continuous Mass Spectrometric Determination of Nitric Oxide in Automotive Exhaust," SAE paper No. 660116, January 1966.
3. Benson, J.D., "Reduction of Nitrogen Oxides in Automobile Exhaust," SAE paper No. 690019, January 1969.
4. "California Air Quality Data II, No. 5," September, October, November, 1970.
5. Cadle, R.D.; and Allen, E.R., "Atmospheric Photochemistry," Science <u>167</u>, No. 3916, January 16, 1970.
6. Lodge, J.P.; and Pate, J.B., Science <u>153</u>, 408, 1966.
7. Junge, C.E., <u>Air Chemistry and Radioactivity</u>, Acad. Press, 1963.
8. "Air Quality Criteria for Hydrocarbons," U.S. Public Health Ser. Publ. No. AP-64, 1970.
9. Leighton, P.A., <u>Photochemistry of Air Pollution</u>, Acad. Press, 1961.
10. "Air Quality Criteria for Hydrocarbons," NAPCA No. AP-64, March 1970.
11. Oberdorfer, P.E., "The Determination of Aldehydes in Automobile Exhaust Gas, SAE Paper No. 670123, January 1967.